

A Foray into Quantum Dynamics¹

By Ross O'Connell, Advisor Professor William Loinaz

1st November 2018

¹Submitted to the Department of Physics of Amherst College in partial fulfillment of the requirements for the degree of Bachelor of Arts with Departmental Honors.

Acknowledgments

First, I thank my parents for being endless sources of love and support. I hope that they appreciate all of the shades of “I wouldn’t be here if it weren’t for you.”

After family, friends. You know who you are. You’ve all lent color and depth to my time here, especially this year.

I must, of course, thank my advisor, Will, for helping me see this problem from all sides, for optimism and enthusiasm. You’ve helped keep this problem from getting me down.

And, finally, Sarah. Because as much as I like my thesis, I go to sleep and wake up thinking of you. As much as I enjoyed working on it, you make me happy.

Abstract

An Explanation of my Thesis in Words of One Syllable

With apologies to Paul Boolos.

My goal for the year was to learn what small things do. If you have a small thing it's not a point, it's a blob – we knew that from the start. But does it stay a blob? No, of course not. It breaks up, but at some time it comes back. At times less than that time, we find small blobs, too. When it's not made of small blobs, the small thing is most odd. It forms lots of hills and troughs. I have ways in here to find out when the blob comes back, where and when the small blobs are, how long it takes for the blobs to break up, where the hills and troughs are, and how many of them there ought to be.

The Same Explanation with Longer Words

The dynamics of a quantum mechanical particle in a time-independent potential are found to contain many interesting phenomena. These are direct consequences of the (typical) existence of more than one time-scale governing the problem. This gives rise to full revivals of initial wavepackets, fractional revivals (multiple wavepackets appearing at fractions of the revival time), and the striking quantum carpets. A variety of analytic techniques are used to consider the interference that gives rise to these phenomena while skirting calculations involving cross-terms. Novel results include a new theorem on

the weighting coefficients a_m that govern fractional revivals, a demonstration that Ψ_{cl} , the function that governs the distribution and features of these fractional revivals, really does behave classically, a treatment of wavepacket dephasing in the infinite square well by means of the Poisson summation formula, and a correct analysis of the spatial distribution of intermode traces. Also, this work presents a coherent treatment of these phenomena, which before now did not exist.

Contents

1	Introduction	7
1.1	A Hitchhiker's Guide to the Infinite Square Well	7
1.1.1	Classical Oscillation and Dispersion	9
1.1.2	Revivals	10
1.1.3	Quantum Carpets	10
1.2	An Analytic Theme: Interference Without Cross-Terms	11
1.3	Semiclassical Physics, Distinctively Quantum Behavior	12
1.4	The Role of Pictures	13
1.5	A Bit of Background	13
2	Quantum Revivals, Full and Fractional	16
2.1	In the Beginning	16
2.2	Fun Revival Facts	17
2.3	Fractional Revivals	21
2.3.1	The General Case	21
2.3.2	A Closer Look at Ψ_{cl} and a_m	29
2.3.3	The Infinite Square Well	32
2.3.4	A Final Note on Ψ_{cl}	34
2.4	Summary	35

<i>CONTENTS</i>	5
3 Quantum Beats	36
3.1 The Early Phase of the Evolution	37
3.2 Fractional Revivals	39
3.3 A Special Case: The Gaussian Distribution	42
3.3.1 Early Evolution	43
3.3.2 Fractional Revivals	45
3.4 A Special Case: The Flat Distribution	46
3.4.1 Early Evolution	47
3.4.2 Fractional Revivals	51
3.5 Summary	53
4 The Connection Between Beats and Carpets	54
4.1 Abuse of the Poisson Summation Formula	55
4.2 A Special Case: Gaussian Weighting Coefficients in the Infinite Square Well	55
4.2.1 Algebra	55
4.2.2 Interpretation	60
4.2.3 A Quick Look at Sech	61
4.2.4 Dephasing of the Wavepacket	64
4.3 Solutions in More Complicated Potentials	67
4.3.1 The WKB Approximation	67
4.3.2 The WKB Approximation and the Poisson Summation Formula	68
4.4 Summary	69
5 Intermode Traces and Quantum Carpets	70
5.1 Multimode Interference	70
5.2 Characteristic Velocities	71
5.3 Characterization of the Velocities	72
5.4 Groups of Velocities and Degeneracy	73

<i>CONTENTS</i>	6
5.4.1 A Quick Example	77
5.5 Degeneracy and Ψ_{cl}	78
5.6 Summary	80
6 Conclusion	83
6.1 Results	83
6.2 Prospects for Future Work	84
A A Few Exactly Solvable Potentials	87
A.1 Old Friends	87
A.1.1 The Infinite Square Well	88
A.1.2 The Simple Harmonic Oscillator	88
A.2 Cousins from the Old Country	89
A.2.1 The Morse Oscillator	89
A.2.2 The Eckart Potential	90
A.2.3 The Pöschl-Teller Potential	91
A.2.4 The Scarf I (Trigonometric) Potential	91
A.2.5 The Scarf II (Hyperbolic) Potential	92
A.2.6 The Rosen-Morse I (Trigonometric) Potential	93
A.2.7 The Rosen-Morse II (Hyperbolic) Potential	94
B Farey Sequences	95
List of Figures	99
Bibliography	104

Chapter 1

Introduction

1.1 A Hitchhiker’s Guide to the Infinite Square Well

The infinite square well is treated in almost every introductory quantum mechanics course. It is the essence of simplicity, a potential bereft of features, its eigenfunctions are simple sine waves. Exact solutions abound. We build an intuition for how quantum mechanical objects should behave, and we move on – after all, the infinite square well is just too simple.

Figure 1.1 was enough to convince me that I didn’t really understand the square well. I had no idea that its probability density was so structured – it hadn’t even occurred to me that it was periodic. So I began the year of study that culminated in this thesis, following much the same pattern as before: look at the square well, find an interesting phenomenon, study it, then see if it occurs in other types of systems¹. While there are applications for most of these phenomena, I won’t pretend that my goal was to find more of them – my goal was to gain a deeper understanding of a fundamental part of quantum mechanics.

¹I focused on time-independent potential wells, in one dimension.

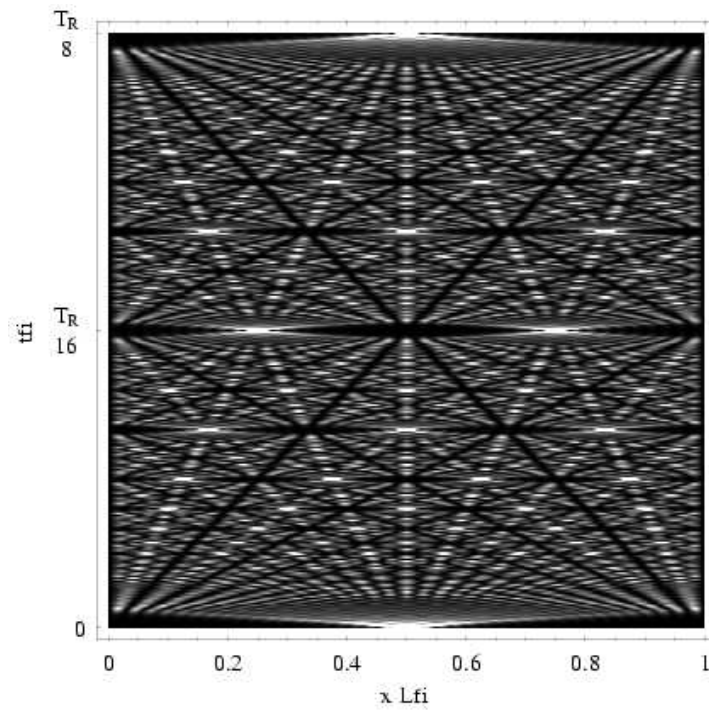
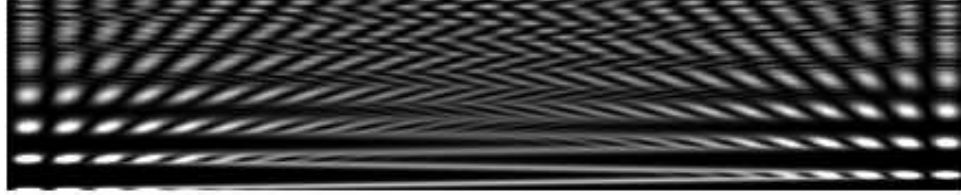


Figure 1.1: A particle in the infinite square well. Lighter areas indicate greater probability density. Our initial wavefunction is a Gaussian packet, centered on $x = L/2$, with $\sigma_x = 0.003L$. For the definition of T_R , see Chapter 2.

1.1.1 Classical Oscillation and Dispersion



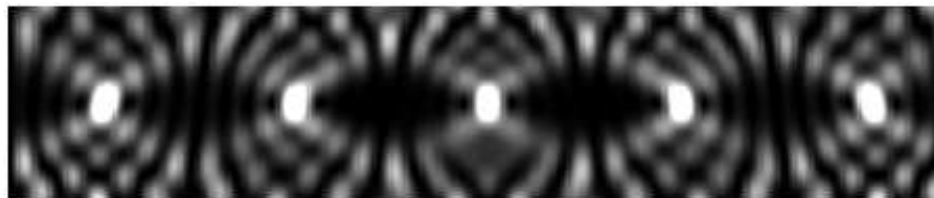
The first interesting phenomenon is that of the classical oscillation of wavepackets. Given a well-localized wavepacket, or even a wavefunction with several distinct peaks, those peaks will undergo something like classical oscillation on a time scale that will be studied in Chapter 2. This is not particularly surprising if we consider Ehrenfest’s Theorem²,

$$\frac{d\langle p \rangle}{dt} = \left\langle -\frac{\partial V}{\partial x} \right\rangle. \quad (1.1)$$

So long as the expectation value of p coincides with the value of p at the center of the wavepacket, the packet’s oscillation will be classical. Of course, this is rarely exactly true and virtually never stays true – when the expectation value of p and the value of p at the center of the wavepacket do not coincide, the wavepacket will begin to disperse, and more characteristically quantum mechanical phenomena will begin to appear. An obvious question to ask is, “can we quantify when this dispersion occurs?” A related question is “does this dispersion occur simultaneously for the whole wavefunction, or does it depend on which point in the wavefunction we are considering?” This question will be considered for a zero-dimensional “quantum beats” system in Chapter 3, and in more dimensions in Chapter 2.

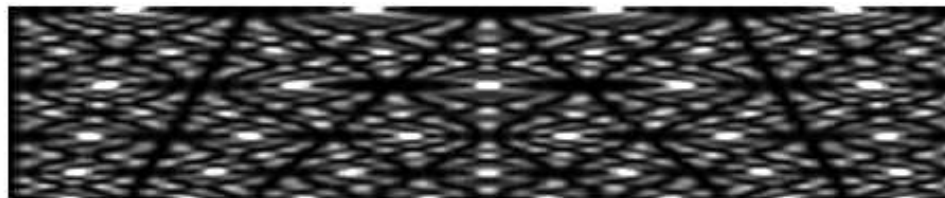
²See [Griffiths, 1995, 17].

1.1.2 Revivals



The next phenomenon that we will consider is closely related to the previous one. It turns out that just as there is a time scale that governs classical oscillation, there is another that governs a distinctly quantum mechanical feature. At this time scale, the original configuration of the wavefunction reappears, in some cases approximately, in others exactly. That is, if we start with a localized wavepacket it will disperse, interfere, and eventually reconstruct itself – what I will call a revival. As part of this process, it will also undergo the same sort of initial classical oscillation that it undergoes immediately after its formation. Stranger still are the existence of fractional revivals, the appearance at times less than the revival time of multiple wavepackets, each related to the original wavepacket. Curiously, both full and fractional revivals became topics of study only recently, even though their existence should be apparent from the $\exp(-iEt/\hbar)$ form of the time evolution terms of the wavefunction. This subject is the focus of Chapter 2, and plays a part in Chapters 3 and 4 as well.

1.1.3 Quantum Carpets



Perhaps the most striking phenomenon is the existence of easily-discerned canals and ridges in the probability density, collections of which have come to be called quantum carpets. While these follow straight lines in the square well, they various curved lines in other potentials. These lines

look much like, but are distinct from, classical trajectories. In Chapter 5 we will see how the two are related. Carpets happen to be, I think, the most difficult phenomena to study. While the revivals problem, and with it the problem of classical oscillation and dispersion, can be reduced to a clever shuffling of phases, it is rather harder to avoid dealing with the entire parameter space of spectrum, eigenfunctions, and particular weighting coefficients. Considering this, it is remarkable that we are able to make interesting statements at all.

1.2 An Analytic Theme: Interference Without Cross-Terms

Last Fall I asked a friend of mine, a math major, if he knew anything about simplifying finite sums. “No,” he replied, “I think you just have to add those up.” The finite sums that I was asking about don’t differ so much from the infinite sums that also appear in this family of problems, and they’re ugly. I was a bit intimidated. One interesting aspect of these problems is that they all pertain to features that we look for *after* “solving” the problem. That is, we start with a set of eigenfunctions, a spectrum, and weighting coefficients, then try to rewrite them to make the features we are interested in manifest. Fortunately, we do have some analytic tools to do this.

All of the phenomena that we are interested in are essentially interference phenomena, produced by the multiplication of two sums. The critical step in every technique presented here is the packaging of the interference information in a form that doesn’t involve cross-terms. These techniques include the grouping of certain parts of the sum by phase (Chapter 2 and 5) and the application of a bit of analysis, the Poisson summation formula (Chapters 3 and 4). Both of these techniques seem initially to make things worse by introducing new sums or integrals, but those new sums and integrals are exactly what give us manageable forms for enough of the interference to make sense of things.

1.3 Semiclassical Physics, Distinctively Quantum Behavior

What exactly constitutes a “semiclassical limit” is not entirely clear. Most of the time, we will take it to mean that the distribution of weighting coefficients n is centered around some central value, \bar{n} , with some characteristic width Δn , and that the hierarchy $1 \ll \Delta n \ll \bar{n}$ holds – i.e. that the packet is localized in physical space. In some cases, we will relax this to the WKB assumption that the potential changes much more slowly than the relevant eigenfunctions oscillate.

It appears that all of the phenomena that I have studied appear most naturally in the study of semiclassical wavepackets. Although the revivals results³ are quite general, they are most striking when we begin with a well-localized initial packet. Otherwise, we just get a mess that occasionally looks like the mess that we started with. Though we are able to solve the infinite square well exactly with each of these techniques (and there $\Delta n \approx \bar{n} \gg 0$ is enough to produce a carpet), our generalizations mostly rely on the WKB approximation. Of course, since we are studying interference phenomena it is not surprising that our most interesting results appear when we have a large number of states that can interfere with each other. Nothing that we have done rules out the appearance of similar phenomena in superpositions of low-energy states, but we have not found any.

What is remarkable is that we find so many distinctly quantum mechanical phenomena in systems that are *supposed* to be becoming more like classical ones. Although we start with wavepackets that are more localized than would be a superposition of, say, the bottom three states in a well, and seem more particle-like, they exhibit bizarre behavior. What is remarkable is that, in the case of carpets, we can use a semiclassical tool to study this.

³In Chapter 3 we will consider the case of quantum beats, a zero-dimensional problem that is interesting even when a small number of states interfere with each other.

1.4 The Role of Pictures

I was able to talk to a lot of people, before my thesis kept me really busy. One evening I was talking with a friend-of-a-friend who happened to be a Chemistry major. She had been through Quantum Chemistry, but was still curious about what things like the uncertainty principle really *meant*. I spent a few minutes waving my hands, then went back to my room and picked up one of my plots of the square well. It proved to be a much more effective way of demonstrating how quantum mechanics can be deterministic, yet still produce so much uncertainty – this pattern *is* the particle in the box. It’s obvious that it doesn’t really have a velocity because it doesn’t even have a trajectory. I think that just as quantum mechanics seems haphazard and riddled with uncertainty until one realizes that the wavefunction is the fundamental object in the theory, pictures seem ill-advised only until one realizes which objects to plot.

I was also attracted to this subject because of a talk that included pictures. There were very few pictures in my otherwise superb quantum mechanics textbook, and as a consequence there were things that I didn’t understand. It didn’t bother me because I didn’t know that I didn’t understand them. The reason that this field developed so recently, and not before, is that these phenomena are immediately apparent in pictures and hopelessly hidden in eigenfunction expansions – and, of course, we couldn’t generate those pictures without computers. I’ve included a lot of pictures in this thesis because I’ve found that while they’re not worth a thousand equations, they’re a fine substitute for a paragraph of my prose.

1.5 A Bit of Background

Much of this thesis is based on three fine papers: the original, authoritative article on fractional revivals, [Averbukh and Perelman, 1989], a strong treatment of quantum beats, [Leichtle et al., 1996b, Leichtle et al., 1996a], and a well-conceived (if roughly executed) paper on intermode traces, [Kaplan et al., 2000, Kaplan et al., 1998].

There are a variety of other papers available. Most studied are revival phenomena, which have

been treated in a variety of ways in a variety of systems. Though the paper mentioned above is remarkable for its clarity and generality, other interesting works include [Aronstein and Stroud, 1997, Aronstein, 2000, Bluhm et al., 1996, Chen and Yeazell, 1998, Jie et al., 1998, Knospe and Schmidt, 1996, Loinaz and Newman, 1999, Razi Naqvi et al., 2001, Rozmej and Arvieu, 1998]. A variety of approaches to quantum carpets have been proposed, though most are restricted to the infinite square well. Some of the more interesting of these involve an analysis in terms of Wigner functions, which I have not pursued. In any case, interesting carpet papers include [Friesch et al., 2000, Grossmann et al., 1997, Hall et al., 2001, Marzoli et al., 1998b, Marzoli et al., 1998a]. For a somewhat dated discussion of some experimental aspects of these phenomena, see [Averbukh and Perelman, 1991].

One of the more intriguing applications of quantum carpet techniques is in the field of Bose-Einstein Condensation. Although I had little time to devote to them, the growing literature suggests that this is a subject of current interest: [Choi et al., 2001, Ruostekoski et al., 2001, Wright et al., 1997].

Papers have been written which study the fractal geometry of various problems, including [Berry, 1996, Wojcik and Zyczkowski, 2001, Wojcik et al., 2000]. The latter two focus on preparing wavepackets that are variations on the Weierstrass function (which everywhere continuous, nowhere differentiable), while the former focuses on the fractal dimension of a particle with a smooth spatial distribution in an n -dimensional box. The most useful insight to come from any of this, I think, is that fractals proper only emerge from initial states that are not proper solutions to the Schrödinger equation. I still suspect that there may be some treatment of carpets that exploits their obvious self-similarity, but the difficulty of fractal proofs combined with the difficulty of working with almost-fractals turned me away from this approach.

There have been attempts to connect the carpet problem to quantum chaos, [Provost and Baranger, 1993, Saif, 2000]. There is a sort of similarity between the phenomena of quantum carpets and chaotic scars (representation of particular classical orbits in the probability densities of a chaotic potential), though little has yet come of this. There is also one paper purporting to connect all of this to quantum computing, [Harter, 2001], though I must confess that I was unable to follow it.

The final connection, which I would have liked to spend more time exploring, is between the prob-

ability density of a quantum mechanical particle in one spatial dimension and electromagnetic wave propagating in two spatial dimensions, in the paraxial approximation. In that field, revivals are instances of the Talbot effect, and fractional revivals instances of the fractional Talbot effect. Apparently, the square well problem, a toy problem in quantum mechanics, translates into a wave guide problem of greater practical importance. For the interested reader, the primary papers on this subject seem to be [Berry and Klein, 1996, Berry and Bodenschatz, 1999, Dubra and Ferrari, 1999, Lock and Andrews, 1992].

Chapter 2

Quantum Revivals, Full and Fractional

2.1 In the Beginning

Our quantum mechanics course began with the Schrödinger equation,

$$i\hbar \frac{\partial \Psi}{\partial t} = -\frac{\hbar^2}{2m} \frac{\partial^2 \Psi}{\partial x^2} + V\Psi, \quad (2.1)$$

and promptly separated it, assuming that the potential V depended only on x :

$$\Psi(x, t) = \psi(x)f(t), \quad (2.2)$$

$$i\hbar \frac{1}{f} \frac{df}{dt} = E, \quad (2.3)$$

$$-\frac{\hbar^2}{2m} \frac{d^2\psi}{dx^2} + V\psi = E\psi. \quad (2.4)$$

Since we could solve Equation 2.3, we did,

$$f(t) = e^{-i\frac{E}{\hbar}t}, \quad (2.5)$$

and turned our attention to the Time-Independent Schrödinger Equation. We quickly found that for bound particles the possible energies E were quantized, making the general solution to the

Schrödinger Equation a weighted sum of the solutions we had found:

$$\Psi(x, t) = \sum_n c_n \psi_n(x) e^{-i \frac{E_n}{\hbar} t}. \quad (2.6)$$

This eigenfunction expansion is useful for algebraic purposes, and admittedly we often want to do things with the wavefunction once we've found it. Unfortunately, the eigenfunction expansion conceals the various interesting things that happen during the time-evolution of a wavefunction. We'll start our analysis of these phenomena with the simplest, quantum revivals.

2.2 Fun Revival Facts

Given a well-localized distribution of weighting coefficients c_n centered around some mean value \bar{n} , we can perform a Taylor expansion¹ of E_n around \bar{n} :

$$E_n \simeq E_{\bar{n}} + E'_{\bar{n}}(n - \bar{n}) + \frac{1}{2!} E''_{\bar{n}}(n - \bar{n})^2 + \frac{1}{3!} E'''_{\bar{n}}(n - \bar{n})^3 + \dots \quad (2.7)$$

We now define

$$\frac{2\pi}{T_j} = \frac{E_{\bar{n}}^{(j)}}{j!}, \quad (2.8)$$

a set of time scales. From these we pick out two important time scales, a classical period $T_{cl} = T_1$ and the revival time $T_R = T_2$. It is the existence of more than one time scale that makes time-evolution in time-independent potentials interesting.

We ignore the $j \geq 3$ terms for two reasons – they make our calculations harder², and in the semiclassical case, which we are most interested in, they really are ignorable. There are two ways

¹From here onward, I will assume that $\hbar^2 = 2m = 1$.

²If we really want to, we could consider the so-called “superrevivals.” These aren't so absurd as to be unobservable, but the big qualitative change in behavior comes from introducing the second time scale, T_R .

to see this. First, we assume that our E_n can be written as a finite sum of weighted powers of n ,

$$E_n = \sum_{m=N}^M d_m n^m. \quad (2.9)$$

This won't always be the case, but I think it's fair to consider transcendental spectra to be unusual.

From looking at E_n , we see that we can write the j th derivative as

$$E_n^{(j)} = \sum_{k=N}^M c_k n^k \times \left(\frac{1}{n^j} \prod_{m=k-j+1}^k m \right). \quad (2.10)$$

We know that the j th characteristic time scale (T_{cl} is the first, T_R is the second) will be proportional to $1/|E_{\bar{n}}^{(j)}|$. We also know that in the semiclassical case, $\bar{n} \gg 1$. If \bar{n} is larger than k , it will force the $E_{\bar{n}}^{(j)}$ terms toward zero, which will in turn force the higher time scales toward infinity. Another way to see this is to realize that the limiting spectrum of any deep potential well is at most n^2 . You can think of this as a consequence of the fact that no well can have walls harder than the infinite square well, but for a more detailed explanation you should consult [Nieto and Simmons, 1979]. Finally, we observe that in the semiclassical limit we are typically concerned with a small region of n -space, within which the first two terms of the Taylor expansion should be an adequate approximation.

To the extent that $T_{cl} \ll T_R$ (which is true in most cases), we can identify two distinct behaviors in the time-evolution of a wavepacket. Writing out our approximate wavefunction³,

$$\Psi(x, t) = \exp(-2\pi i E_{\bar{n}} t) \sum_n c_n \psi_n(x) \exp \left[-2\pi i \left(\frac{(n - \bar{n})t}{T_{cl}} + \frac{(n - \bar{n})^2 t}{T_R} \right) \right], \quad (2.11)$$

we can see that when $t \approx T_{cl}$, the t/T_R term will make no significant contribution to the time-evolution, and the wavefunction will oscillate classically with period T_{cl} . With time the t/T_R term causes the wavepacket to disperse, and interference between the various states produces a quantum carpet. However, as t approaches within a few T_{cl} of T_R , the t/T_R term contribution again becomes

³Note that we are writing our wavefunction as a function of \vec{x} rather than as a function of x . This is because when considering revival problems, we aren't particularly concerned about the dimensionality of the wavefunction. We *will* be concerned about this in subsequent chapters, and when we are the arrow will come off of the x .

small and the wavepacket returns to classical oscillation. When $t = T_R$, a quantum revival occurs. If T_R is an integer multiple of T_{cl} , the wavefunction returns to its original configuration, and if not then it returns to something very close to its original configuration.

This is illustrated in Figure 2.1, where we see the initial evolution of a particle in an infinite square well of width a . We use a Gaussian distribution of weighting coefficients with $\bar{n} = 40$ and $\sigma_n = 2$,

$$c_{\bar{n}+k} = \frac{1}{\sigma_n \sqrt{2\pi}} e^{-k^2/2\sigma_n^2}. \quad (2.12)$$

Referring to Equation 2.8 and Section A.1.1, we can calculate the time scales for the square well,

$$T_{cl} = \frac{L^2}{\bar{n}\pi}, \quad (2.13)$$

$$T_R = \frac{2L^2}{\pi}, \quad (2.14)$$

and find that $T_R = 80T_{cl}$. We can see clearly the initial classical oscillation of the particle (the oscillations are straight lines, as we would expect in the square well) and its subsequent dispersion and interference. Note that the periods of the oscillations, so long as they are well-defined, are T_{cl} .

Finally, we may note that in cases where the spectrum is strictly linear in n , such as the simple harmonic oscillator, we would (from this analysis) expect no dispersion, little to no interference, no quantum carpet – just classical oscillation. Though this is not entirely true, it is roughly true in virtually all cases⁴. An example of classical oscillation is shown in Figure 2.2. There, $\bar{n} = 5$ and $\sigma_n = 2$.

We also find revival-esque phenomena at $t < T_R$. If we examine $\|\Psi\|^2$ at a few particular times in the infinite square well, as in Figure (insert figure ISW-Cuts)2.3, we notice something interesting. At $t = T_R/2$, $\|\Psi(x,0)\|^2$ has been reflected about the center of the well, and at $t = T_R/4$ there are two copies of the original probability distribution, one reflected about the center of the well. Although this particular result does not hold generally⁵, it may suggest to us that interesting things

⁴In Chapter 5 we will learn the black art of “quadrating spectra,” which will let us make wavefunctions with carpets in problems with linear spectra.

⁵For this result to hold we require eigenstates of definite parity and a purely quadratic spectrum. For a discussion

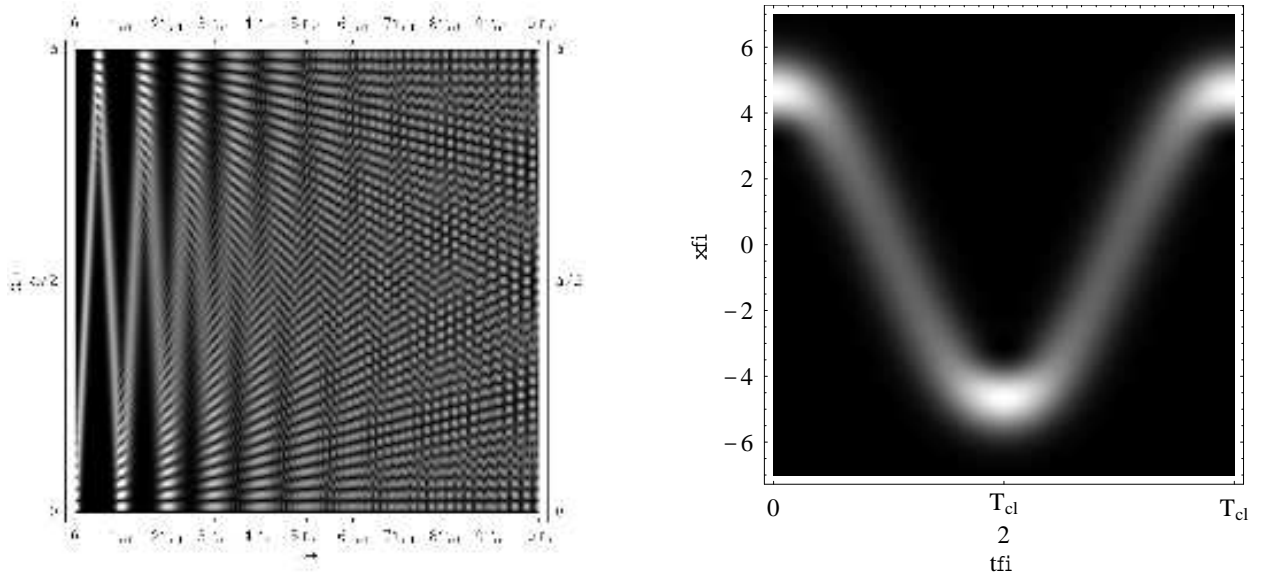


Figure 2.1: $\|\Psi\|^2$ for a particle in an infinite square well, such that $T_R = 80T_{cl}$. The distribution of coefficients is Gaussian, with $\bar{n} = 40$ and $\sigma_n = 2$. For the form of the square well that I am using, see Section A.1.1.

Figure 2.2: $\|\Psi\|^2$ for a simple harmonic oscillator. The distribution of coefficients is Gaussian, with $\bar{n} = 6$ and $\sigma_n = 2$. For the version of the simple harmonic oscillator that I am using, see Section A.1.2.

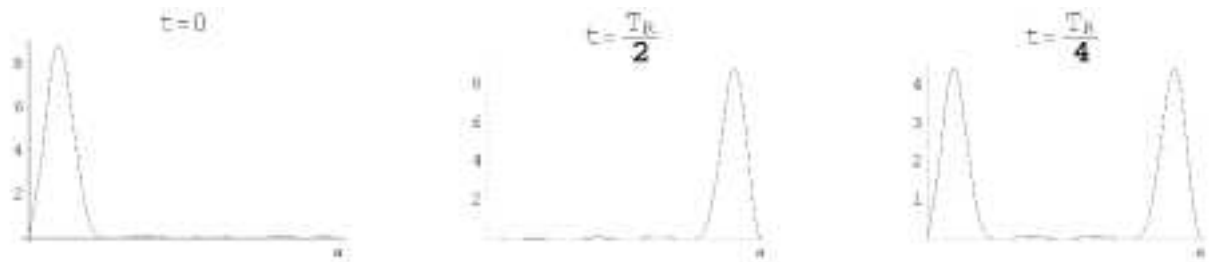


Figure 2.3: Plots of $\|\Psi\|^2$ for a particle in an infinite square well at $t = 0$, $t = T_R/2$, and $t = T_R/4$. Note that the scale is different for the rightmost plot – though conservation of probability shrinks our peaks, they have the same shape as the peaks in the other two plots.

happen at rational fractions of the revival time.

2.3 Fractional Revivals

We have seen the existence of revivals – times when the original wavefunction perfectly or near-perfectly reassembles itself. We have also seen that in at least one case we can find revival-like phenomena at $t \ll T_R$. Indeed, if we look at Figure 2.4, we might suspect that something interesting happens at most rational fractions of T_R . It turns out that while perfect revivals⁶ at times other than the revival time are rather unusual, an initial wavepacket will give rise to arrays of other packets (which are not, in general, identical to the original packet) at rational fractions of T_R . The motivation for this is more algebraic than physical – it has to do with our ability at rational fractions of T_R to group together states with the same phase. This phenomenon was treated quite definitively in [Averbukh and Perelman, 1989], and the next section will closely follow their derivation.

2.3.1 The General Case

In this section, we will restrict ourselves to wavefunctions that can be well-approximated by the following⁷:

$$\Psi(\vec{x}, t) = \sum_{k=-\infty}^{\infty} c_{(k+\bar{n})} \psi_{(k+\bar{n})}(\vec{x}) \exp -2\pi i \left(k \frac{t}{T_{cl}} + k^2 \frac{t}{T_R} \right), \quad k = n - \bar{n} \quad (2.15)$$

This is a fairly large class of problems - virtually any problem with a well-localized distribution of c_n around some mean value \bar{n} , and any problem in a potential with a quadratic spectrum. This derivation makes no assumptions about the dimensionality of the problem, but does assume that the spectrum is a function of only one quantum number. Though we don't believe the generalization of these exact fractional revivals, see [Loinaz and Newman, 1999].

⁶See [Loinaz and Newman, 1999] for a discussion of such revivals.

⁷We apologize in advance for the lower limit on the sum, which should only go to $-\bar{n}$. The idea is that while all the $k < -\bar{n}$ terms should have weightings of *exactly* zero, we can make the approximation that their weighting coefficients are very small. For some sums and integrals these limits will greatly simplify our calculation. We've also dropped the leading $\exp(-2\pi i E_{\bar{n}} t)$ term, as it has no impact on the relative phase of the various eigenfunctions and thus no physical significance.

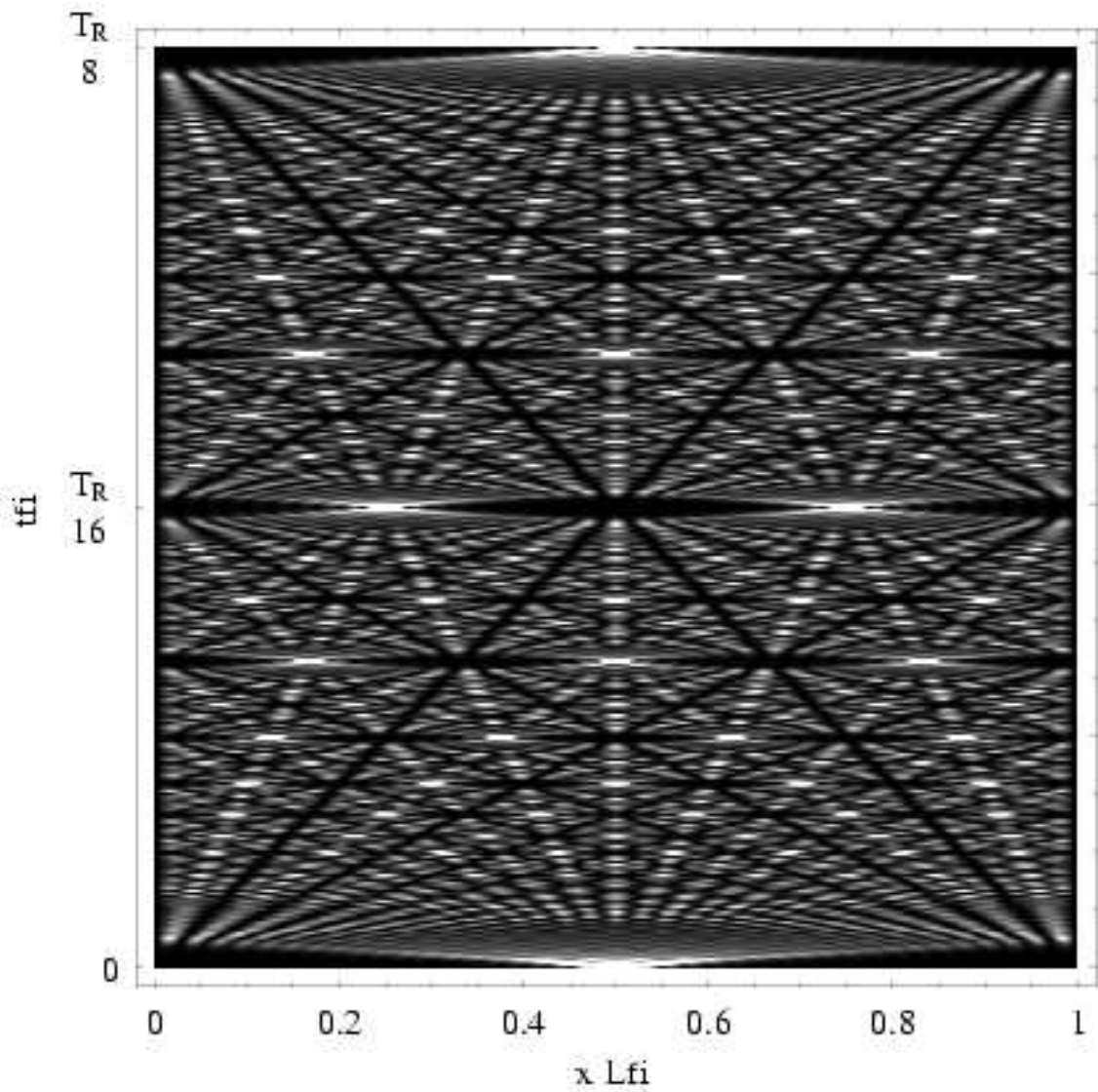


Figure 2.4: Fractional revivals in the infinite square well. Our initial wavefunction is a Gaussian packet, centered on $x = L/2$, with $\sigma_x = 0.003L$. The symmetry of our wavepacket allows it to have a full revival (modulo an overall phase factor) at $t = T_R/8$. At times below that, though, we should be able to count the fractional revivals.

to more variables to be particularly problematic, we have not considered it here.

We will look at the wavefunction at rational fractions of the revival time, $t = \frac{p}{q}T_R$, where $p, q \in \mathbb{Z}$ and p and q are relatively prime⁸. At such times we might expect that the t/T_R terms in the time evolution will reduce to some set of rational numbers, and that many values of k will have the same phase contributions. We will begin by looking only at exact times, but will find that our result is also a good approximation at $t = \frac{p}{q}T_R + \Delta t$.

If we now define

$$\phi_k = \frac{p}{q}k^2 \bmod 1, \quad (2.16)$$

which characterizes the deviation in phase of each eigenfunction from classical oscillation, we can write

$$\Psi(\vec{x}, t = \frac{p}{q}T_R) = \sum_{k=-\infty}^{\infty} c_k \psi_x(\vec{x}) \exp\left(-2\pi i \left(k \frac{p}{q} \frac{T_R}{T_{cl}} + \phi_k\right)\right). \quad (2.17)$$

Now, consider the conditions for some of these phases to match. If we can collect the terms of the sum into a handful of equivalence classes (defining two terms as equivalent when they have identical ϕ_k), we can turn the infinite sum over k into a finite sum over another variable⁹. This is a question about the periodicity of ϕ_k which can be easily answered. We are looking for the minimal l such that $p, q \in \mathbb{Z}$ and for all k ,

$$\begin{aligned} \phi_k &= \phi_{k+l} \\ \frac{p}{q}k^2 \bmod 1 &= \frac{p}{q}(k+l)^2 \bmod 1. \end{aligned} \quad (2.18)$$

This leads us to two conditions on l ,

$$\frac{2pl}{q} \in \mathbb{Z}, \quad (2.19)$$

$$\frac{pl^2}{q} \in \mathbb{Z}. \quad (2.20)$$

⁸This relatively prime business is going to force the set of revivals that we can resolve to fit a Farey sequence. For more on this, see Appendix B or [Harter, 2001] or [Weisstein, 1999].

⁹Well, that finite sum is itself over another infinite sum, but since when did you get something for nothing?

There are two important solutions to Equation 2.19, $l = q$ and $l = q/2$. Our task is to find out when the $l = q/2$ is consistent with 2.20, and when the minimal value of l is just q . There are three cases here for us to consider,

Case 1: q is odd

For odd q , $l = q$. While $l = q/2$ would satisfy Equation 2.19, $q/2$ is not an integer, as we require.

Case 2: q contains more than one power of 2

When q contains more than one power of 2, $l = q/2$. This obviously satisfies Equation 2.19, and Equation 2.20 reduces to $pq/4 \in \mathbb{Z}$, which is also true.

Case 3: q contains only one power of 2

If q contains only one power of 2, $l = q$. While $l = q/2$ satisfies Equation 2.19, it does not satisfy Equation 2.20. That would require that $pq/4 \in \mathbb{Z}$, but since p and q are relatively prime, p must be odd, and by assumption $q/4$ is half-integer.

We have established that ϕ_k is periodic, and we will be able to turn our sum over k into a sum with l terms. Note that if we were to consider times that were not rational fractions of T_R , we would be able to group the phase contributions from the k^2 term. With this relationship in hand, we may make a guess about how we may rewrite the wavefunction. Let us first define

$$\Psi_{cl}(\vec{x}, t) = \sum_{k=-\infty}^{\infty} c_k \psi_k(\vec{x}) \exp\left(-2\pi i k \frac{t}{T_{cl}}\right), \quad (2.21)$$

a version of the wavefunction with the “dispersion” terms removed. We postulate that we can then

write the wavefunction as a weighted sum of time-slices¹⁰ of Ψ_{cl} ,

$$\Psi\left(\vec{x}, t = \frac{p}{q}T_R\right) = \sum_{s=0}^{l-1} a_s \Psi_{cl}\left(\vec{x}, \frac{p}{q}T_R + \frac{s}{l}T_{cl}\right). \quad (2.22)$$

We will now demonstrate that Equation 2.22 is valid by explicit construction of the coefficients a_s .

First, we plug Equation 2.21 into Equation 2.22,

$$\begin{aligned} \Psi(x, t = \frac{p}{q}T_R) &= \sum_{s=0}^{l-1} a_s \Psi_{cl}\left(\vec{x}, t + \frac{s}{l}T_{cl}\right) \\ &= \sum_{s=0}^{l-1} a_s \sum_{k=-\infty}^{\infty} c_k \psi_k(\vec{x}) \exp\left(-2\pi i k \frac{t + (s/l)T_{cl}}{T_{cl}}\right) \\ &= \sum_{k=-\infty}^{\infty} c_k \psi_k(\vec{x}) \exp\left(-2\pi i k \frac{t}{T_{cl}}\right) \sum_{s=0}^{l-1} a_s \exp\left(-2\pi i \frac{s}{l}k\right). \end{aligned} \quad (2.23)$$

We now compare the result with Equation 2.17 and arrive at the condition

$$\exp(-2\pi i \phi_k) = \sum_{s=0}^{l-1} a_s \exp\left(-2\pi i \frac{s}{l}k\right), \quad (2.24)$$

for $k = 0, 1, \dots, l-1$.

We now need to find an explicit expression for the constants a_s . If we multiply Equation 2.24 by $\exp(2\pi i \frac{m}{l}k)$, where m is an integer, and sum over k , we can use the completeness relation of the Fourier sum to extract the coefficient:

¹⁰Recall that the rational numbers form a dense subset of the real numbers. This means that we can approximate the wavefunction arbitrarily well at any value of t with slices of Ψ_{cl} , which in turn implies that the set of time slices of Ψ_{cl} taken at rational times form a basis for the Hilbert space of a particular problem. This was first observed in [Aronstein and Stroud, 1997].

$$\begin{aligned} \sum_{k=0}^{l-1} e^{-2\pi i(\phi_k - \frac{m}{l}k)} &= \sum_{k=0}^{l-1} \sum_{s=0}^{l-1} a_s e^{-2\pi i \frac{s-m}{l}k} \\ &= l \sum_{s=0}^{l-1} a_s \delta_{s,m}, \end{aligned} \quad (2.25)$$

$$a_m = \frac{1}{l} \sum_{k=0}^{l-1} e^{-2\pi i(\phi_k - \frac{m}{l}k)}. \quad (2.26)$$

We have constructed the a_s , but we can rewrite equation (2.26) in a form more conducive to computation. First, we define how we will step through the possible values of m :

$$m' = (m + 2\frac{pl}{q}) \bmod l. \quad (2.27)$$

With this in place, we are prepared to derive the following:

$$\begin{aligned} a_{m'} \exp\left(-2\pi i \left(\frac{m}{l} + \frac{p}{q}\right)\right) &= \frac{1}{l} \exp\left(-2\pi i \left(\frac{m}{l} + \frac{p}{q}\right)\right) \sum_{k=0}^{l-1} \exp\left(-2\pi i \left(\frac{p}{q}k^2 - \frac{m}{l}k - \frac{p}{q}2k\right)\right) \\ &= \frac{1}{l} \sum_{k=0}^{l-1} \exp\left(-2\pi i \left(\frac{p}{q}(k-1)^2 - \frac{m}{l}(k-1)\right)\right), \end{aligned} \quad (2.28)$$

from which, shifting the summation index by 1, exploiting the periodicity of ϕ_k , and rearranging the equation for convenience, we conclude

$$a_{m'} = a_m e^{2\pi i \left(\frac{m}{l} + \frac{p}{q}\right)}. \quad (2.29)$$

It is easily confirmed that when q is odd or contains more than one power of 2, the a_m 's with $m = l$ and $m = 2\frac{pl}{q}$ will have opposite parity, and all of the a_m will have the same modulus. When q contains only one power of two, both a_m for $m = l$ and $m = 2\frac{pl}{q}$ will be even, and the coefficients with even and odd indices will have different moduli. As it happens, the coefficients with even

indices are all zero.

Now, let us compare our result with the actual wavefunction at $t = \frac{p}{q}T_R + \Delta t$. The actual wavefunction is

$$\Psi\left(\vec{x}, \frac{p}{q}T_R + \Delta t\right) = \sum_{k=-\infty}^{\infty} c_k \psi_k(\vec{x}) \exp -2\pi i \left(\frac{p}{q} \frac{T_R}{T_{cl}} k + \frac{\Delta t}{T_{cl}} k + \frac{p}{q} k^2 + \frac{\Delta t}{T_R} k^2 \right). \quad (2.30)$$

Using Equations 2.23 and 2.24, we find that

$$\Psi\left(\vec{x}, t = \frac{p}{q}T_R + \Delta t\right) = \sum_{s=0}^{l-1} a_s \Psi_{cl}\left(\vec{x}, \frac{p}{q}T_R + \Delta t + \frac{s}{l}T_{cl}\right) \quad (2.31)$$

$$= \sum_{k=-\infty}^{\infty} \sum_{s=0}^{l-1} a_s \exp\left(-2\pi i \frac{s}{l} k\right) c_k \psi_k(\vec{x}) \exp -2\pi i \left(\frac{p}{q} \frac{T_R}{T_{cl}} k + \frac{\Delta t}{T_{cl}} k \right) \quad (2.32)$$

$$= \sum_{k=-\infty}^{\infty} c_k \psi_k(\vec{x}) \exp -2\pi i \left(\frac{p}{q} \frac{T_R}{T_{cl}} k + \frac{\Delta t}{T_{cl}} k + \frac{p}{q} k^2 \right), \quad (2.33)$$

which will be a good approximation so long as $k\Delta t/T_R \ll \Delta t/T_{cl}$, where we must consider the largest “relevant” k . This is, perhaps, a closer correspondence than we should really expect – remember that at the start of this derivation we only required that our rewriting of the wavefunction be equivalent to it at $t = (p/q)T_R$.

We may ask what this means for $\|\Psi\|^2$. At a rational fraction of the revival time, we have

$$\left\| \Psi\left(x, t = \frac{p}{q}T_R\right) \right\|^2 = \sum_{s,z=0}^{l-1} a_s a_z^* \Psi_{cl}\left(\vec{x}, \frac{p}{q}T_R + \frac{s}{l}T_{cl}\right) \Psi_{cl}^*\left(\vec{x}, \frac{p}{q}T_R + \frac{z}{l}T_{cl}\right), \quad (2.34)$$

a product of several time-slices of Ψ_{cl} . In cases where we didn’t have a well-defined wavepacket to begin with, or in the case where Ψ_{cl} doesn’t preserve this wavepacket, we should not expect discernible fractional revivals. However, to the extent that each slice of Ψ_{cl} contains a peak that has no significant overlap with any of the other time-slices in question, the cross-terms in the sum will make a negligible contribution and we will have several well-defined wavepackets - a fractional revival. To see this, consult Figure 2.4, where you should be able to count the fractional revivals.

Of course, we have (as of yet) no guarantee that Ψ_{cl} is really free of dispersion, or that wavepackets really follow their classical paths. Though we have attached the label of “classical” to Ψ_{cl} and T_{cl} , we have yet to prove anything about them – that will have to wait for Section 5.5, when we’ve developed a technique for analyzing interference in quantum carpets. Before then, though, we can present some highly suggestive pictures, Figures 2.5 and 2.6.

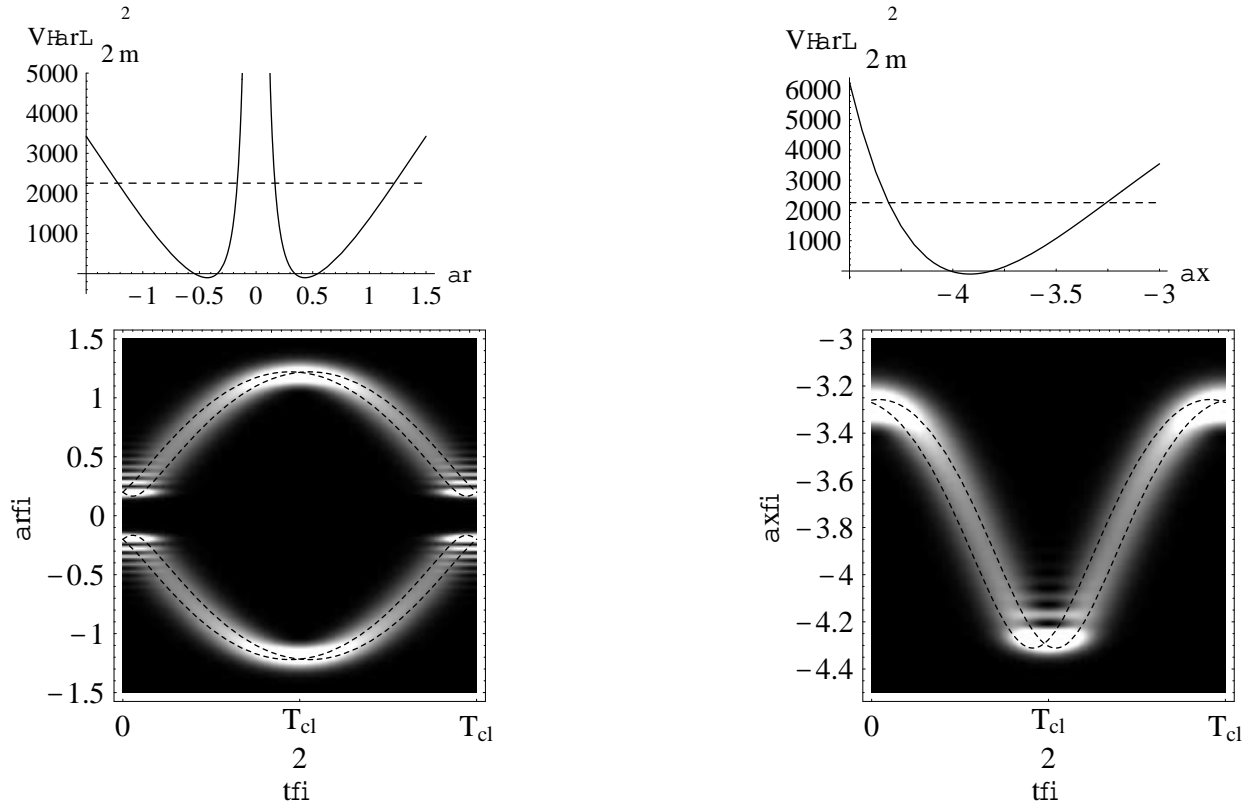


Figure 2.5: $V(\alpha r)$ (above) and $\|\Psi_{cl}\|^2$ (below) for a particle in the Pöschl-Teller potential (see Appendix A). The dotted line in the above plot indicates $E_{\bar{n}}$, in the lower plot they indicate four different classical paths of energy $E_{\bar{n}}$. The Pöschl-Teller potential has a purely quadratic spectrum. For more details on it, see Section A.2.3.

Figure 2.6: $V(\alpha x)$ (above) and $\|\Psi_{cl}\|^2$ (below) for a particle in the Morse potential (see Appendix A). The dotted line in the above plot indicates $E_{\bar{n}}$, in the lower plot they indicate four different classical paths of energy $E_{\bar{n}}$. The Morse potential has a purely quadratic spectrum. For more details on it, see Section A.2.1.

2.3.2 A Closer Look at Ψ_{cl} and a_m

If you take a moment to write down the particular a_m for some p/q , you will find that all values in question appear twice¹¹. For example, at $p/q = 1/5$ we find

$$a_0 = a_0, \quad (2.35)$$

$$a_2 = a_0 \exp\left(-2\pi i \frac{1}{5}\right), \quad (2.36)$$

$$a_4 = a_0 \exp\left(-2\pi i \frac{4}{5}\right), \quad (2.37)$$

$$a_1 = a_0 \exp\left(-2\pi i \frac{4}{5}\right), \quad (2.38)$$

$$a_3 = a_0 \exp\left(-2\pi i \frac{1}{5}\right). \quad (2.39)$$

Of course, we can find a reason for this. Let us suppose that from Equation 2.27 we can construct a function $m(n)$ such that $m(0) \equiv 0$ and $m(-n) \equiv m(l-n)$. If this is true, we can further simplify our expression for fractional revivals. Obviously, $m(n)$ would depend on whether l was odd, a multiple of more than one power of two, or an odd multiple of two, so we will have to perform this analysis for three different cases. Fortunately, the proof that these a_m 's come in pairs follows the same outline in each case. First, we will confirm that $(m(n) + m(-n)) \bmod l = 0$, which will tell us that $a_{m(n)}$ and $a_{m(-n)}$ connect $\Psi_{cl}(\vec{x}, t + \Delta t)$ and $\Psi_{cl}(\vec{x}, t - \Delta t)$ (see Equation 2.22). Second, we will prove that $a_{m(n)} = a_{m(-n)}$, to see if we could further simplify the sum in Equation 2.22. This is to be done by induction - since $a_{m(0)} = a_{m(-0)}$, if $a_{m(n)} = a_{m(-n)}$ implies $a_{m(n+1)} = a_{m(-n-1)}$ then $a_{m(n)} = a_{m(-n)}$ for all n .

From Equation 2.29, we know that

$$a_{m(n+1)} = a_{m(n)} \exp 2\pi i \left(\frac{m(n)}{l} + \frac{p}{q} \right), \quad (2.40)$$

¹¹While the explicit examples that they calculated reflected the results of this section, Averbukh and Perelman did not state or use them.

and if we change the sign of n and shift the indices by one we can rearrange this to read

$$a_{m(-n-1)} = a_{m(-n)} \exp -2\pi i \left(\frac{m(-n-1)}{l} + \frac{p}{q} \right). \quad (2.41)$$

Using our inductive hypothesis, $a_{m(n)} = a_{m(-n)}$, we need only show that

$$\frac{-m(-n-1)}{l} = \frac{m(n)}{l} + 2\frac{p}{q}. \quad (2.42)$$

If all of this holds, we can define

$$h \equiv \begin{cases} \frac{l-1}{2}, & l \text{ odd,} \\ \frac{l}{2}, & l \text{ even,} \end{cases} \quad (2.43)$$

and rewrite Equation 2.22 as

$$\Psi \left(\vec{x}, t = \frac{p}{q} T_R \right) = \sum_{s=0}^h a_s \left(\Psi_{cl} \left(\vec{x}, \frac{p}{q} T_R + \frac{s}{l} T_{cl} \right) + \Psi_{cl} \left(\vec{x}, \frac{p}{q} T_R - \frac{s}{l} T_{cl} \right) \right). \quad (2.44)$$

Let's examine the three cases:

Case 1: q is odd

If q is odd, then $l = q$, and $m' = (m + 2p) \bmod q$, from which we can deduce

$$m(n) = 2pn \bmod q, \quad (2.45)$$

$$a_{m(n)} = a_0 \exp 2\pi i \left(n \frac{p}{q} + \sum_{N=0}^{n-1} \frac{2pn \bmod q}{q} \right). \quad (2.46)$$

The definition $m(-n) \equiv -2pn \bmod q$ is consistent with our condition that $m(-n) = m(l - n)$.

Moreover, under this definition $m(n) + m(-n) = 0$, satisfying our first condition. Turning our

attention to Equation 2.42, we see that

$$\begin{aligned}
\frac{-m(-n-1)}{l} &= \frac{-(-2pn-2p) \bmod q}{q} \\
&= \frac{2pn}{q} \bmod q + \frac{2p}{q} \\
&= \frac{m(n)}{l} + 2\frac{p}{q},
\end{aligned} \tag{2.47}$$

and our theorem holds.

Case 2: q contains more than one power of 2

If q contains more than one power of 2, then $l = q/2$, and $m' = (m+p) \bmod q/2$. We may then say that

$$m(n) = pn \bmod q/2, \tag{2.48}$$

$$a_{m(n)} = a_0 \exp 2\pi i \left(n\frac{p}{q} + \sum_{N=0}^{n-1} \frac{pn \bmod q/2}{q/2} \right). \tag{2.49}$$

The definition $m(-n) \equiv -pn \bmod q/2$ is consistent with our condition that $m(-n) = m(l-n)$. Moreover, under this definition $m(n) + m(-n) = 0$, satisfying our first condition. Turning our attention to Equation 2.42, we see that

$$\begin{aligned}
\frac{-m(-n-1)}{l} &= \frac{-(-pn-p) \bmod q}{q/2} \\
&= \frac{pn}{q/2} \bmod q + \frac{2p}{q} \\
&= \frac{m(n)}{l} + 2\frac{p}{q},
\end{aligned} \tag{2.50}$$

and our theorem holds again.

Case 3: q contains only one power of 2

If q contains only one power of two, then again $l = p$. The principle difference from the q -odd case is that $a_0 = 0$, while a_1 is non-zero. The proof in the q -odd case holds for the odd m , while for even m , $a_m = 0$, and we may easily define $a_{l-m} = 0$. Thus our theorem holds in this final case.

2.3.3 The Infinite Square Well

Equation 2.44 is particularly useful when we can find some connection between the paired slices of Ψ_{cl} . The eigenfunctions of the infinite square well are harmonic functions, particularly easy to combine with the time evolution term in both Ψ and Ψ_{cl} . Perhaps the first thing to do is plot a particular example – Figure 2.7 shows what looks like two wave packets bouncing off the walls of the well.

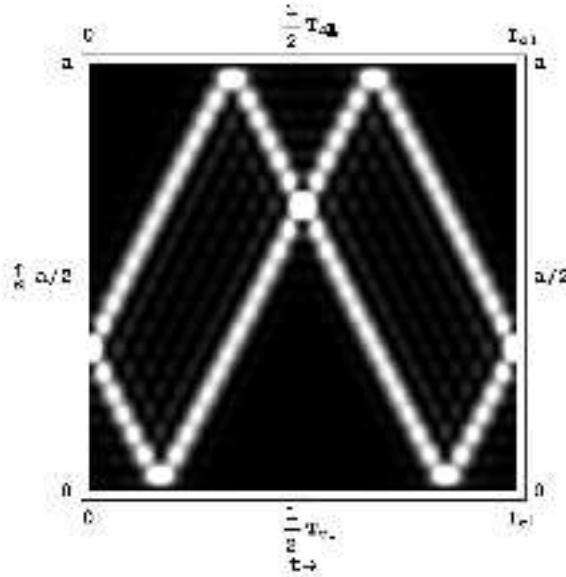


Figure 2.7: Ψ_{cl} for a roughly Gaussian spatial distribution, centered at $x = a/3$.

We start out from equation (2.21) and fill in the specifics of the problem:

$$\Psi_{cl}(x, t) = \sum_{k=-\infty}^{\infty} c_{(k+\bar{n})} \sqrt{\frac{2}{L}} \sin\left(\frac{(k+\bar{n})\pi}{L}x\right) \exp\left(-2\pi i k \frac{t}{T_{cl}}\right). \quad (2.51)$$

We then rewrite the sine terms as a sum of exponentials,

$$\begin{aligned}
\Psi_{cl}(x, t) &= \sum_{k=-\infty}^{\infty} c_k \sqrt{\frac{2}{L}} \frac{i}{2} \left(\exp\left(i \frac{k\pi}{L} x\right) - \exp\left(-i \frac{k\pi}{L} x\right) \right) \exp\left(-2\pi i k \frac{t}{T_{cl}}\right) \\
&= \sum_{k=-\infty}^{\infty} c_k \sqrt{\frac{2}{L}} \frac{i}{2} \left(\exp i \frac{k\pi}{L} \left(x - \frac{2L}{T_{cl}} t\right) - \exp -i \frac{k\pi}{L} \left(x + \frac{2L}{T_{cl}} t\right) \right) \\
&= \sum_{k=-\infty}^{\infty} c_k \sqrt{\frac{2}{L}} \frac{1}{2} \left(\sin \frac{k\pi}{L} \left(x - \frac{2L}{T_{cl}} t\right) + \sin \frac{k\pi}{L} \left(x + \frac{2L}{T_{cl}} t\right) \right. \\
&\quad \left. + i \cos \frac{k\pi}{L} \left(x - \frac{2L}{T_{cl}} t\right) - i \cos \frac{k\pi}{L} \left(x + \frac{2L}{T_{cl}} t\right) \right). \tag{2.52}
\end{aligned}$$

Note that $\frac{2L}{T_{cl}}$ is the velocity associated with classical motion in the square well. If we plug in $t = \frac{p}{q} T_R \pm \frac{s}{l} T_{cl}$, we find that we can rewrite the arguments of the trigonometric functions as $\left(x + \frac{2Lp}{q} \frac{T_R}{T_{cl}}\right) \pm 2L \frac{s}{l}$. Now, inserting Equation 2.52 into Equation 2.44, we find

$$\begin{aligned}
\Psi(\vec{x}, t = \frac{p}{q} T_R) &= \sum_{s=0}^h a_s \sum_{k=-\infty}^{\infty} c_k \sqrt{\frac{2}{L}} \left(\sin \frac{k\pi}{L} \left(x - \frac{2L}{T_{cl}} \frac{s}{l} T_{cl}\right) + \sin \frac{k\pi}{L} \left(x + \frac{2L}{T_{cl}} \frac{s}{l} T_{cl}\right) \right) \\
&= \sum_{s=0}^h a_s (\Psi(x - \Delta x_s, 0) + \Psi(x + \Delta x_s, 0)), \tag{2.53}
\end{aligned}$$

where we have defined $\Delta x_s = 2L \frac{s}{l}$.

It is rather surprising that in the infinite square well, at any rational fraction of the revival time, the wavefunction can be treated as a weighted sum of translations of the initial wavefunction. Note that $\Psi(-x, 0) = \Psi(2L - x, 0) = -\Psi(x, 0)$, which ensures that each pair of translations will meet the boundary conditions of the square well - indeed, these translations can be thought of as disturbances in a dispersionless string, with the leftward (rightward) translation contributing the π -phase-shifted reflection of the rightward (leftward) translation.

The result that all fractional revivals in the square well consist of translated copies of the original wavefunction was stated but not proven in [Aronstein and Stroud, 1997]. There, the analogy with the dispersionless string is simply asserted, and the translations derived from that.

This impressively simple result is, of course, a direct consequence of the overwhelming simplicity

of the infinite square well. That does not mean, however, that we cannot gain important physical insight from this result. We can think of Ψ_{cl} as not changing shape during its time-evolution because there are no features on the bottom of the well. We might then guess that the degree of dispersion, and thus the degree to which the fractional revivals do not resemble the original wavepacket, depends on the features of the potential.

2.3.4 A Final Note on Ψ_{cl}

Obviously, Ψ_{cl} does not satisfy the Schrödinger equation – can we find a similar equation that it *does* satisfy? We can examine a few derivatives, and see if we can reconstruct something analogous to the Schrödinger equation. First, referring to equation 2.21, defining $E \equiv |E'_n|$ we can calculate the following derivatives:

$$\frac{\partial \Psi_{cl}}{\partial t} = \sum_k c_k \psi_k (-iEk) e^{-iEkt} \quad (2.54)$$

$$\frac{\partial^2 \Psi_{cl}}{\partial x^2} = \sum_k c_k \frac{\partial^2 \psi_k}{\partial x^2} e^{-iEkt}. \quad (2.55)$$

Invoking the Time-Independent Schrödinger Equation, $E_k \psi_k = -\frac{\partial^2 \psi_k}{\partial x^2} + V \psi_k$, we can find

$$\begin{aligned} \frac{\partial^2 \Psi_{cl}}{\partial x^2} &= \sum_k c_k (V - E_k) \psi_k e^{-iEkt} \\ &= V \Psi_{cl} - \sum_k c_k E_k \psi_k e^{-iEkt} \\ &= V \Psi_{cl} - i \frac{\partial \Psi_{cl}}{\partial t} - \sum_k c_k (E_k - Ek) \psi_k e^{-iEkt}, \end{aligned} \quad (2.56)$$

which we can rearrange to the following Schrödinger-like equation:

$$i \frac{\partial \Psi_{cl}}{\partial t} = -\frac{\partial^2 \Psi_{cl}}{\partial x^2} + V \Psi_{cl} - \sum_k c_k (E_k - Ek) \psi_k e^{-iEkt}. \quad (2.57)$$

Brief examination of Equation 2.57 should reveal why this did not prove to be a successful vein of analysis. We have lost linearity, one of the most attractive features of the Schrödinger equation.

2.4 Summary

One of the principal differences between classical and quantum mechanics is that quantum systems have more than one time scale. Because of this, we can find many interesting phenomena in their time-evolution. In this chapter, we saw that the phenomenon of full and fractional revivals are quite general consequences of weighted sums of complex exponentials. We have also seen that we can express fractional revivals of a wavefunction as a weighted sum of a “classicized” wavefunction, Ψ_{cl} – regardless of the original spectrum, we give Ψ_{cl} a linear spectrum, greatly simplifying *its* evolution. A new relationship between the weighting coefficients in that sum, a_m and a_{-m} , was proved, leading to a proof that fractional revivals in the infinite square well are simply translations and reflections of the original wavefunction.

Chapter 3

Quantum Beats

The object of consideration in this chapter¹ is a weighted sum of exponentials,

$$f(t) = \sum_n P_n e^{iE(n)t}. \quad (3.1)$$

As one might expect, these sorts of sums exhibit revival phenomena just as in the previous chapter, when the P_n were functions. In the literature, this sort of sum is said to produce “quantum beats,” and they are important because many laboratory measurements are of signals that can be written in this form – for example, the fluorescence of an ensemble of atoms, each excited to one of a few almost identical energy levels. This is a useful enough phenomenon to have given rise to techniques such as quantum beat spectroscopy². Because this is effectively a zero dimensional problem, there are fewer dynamical features for us to consider. Because of the weighted exponential form, we will see revivals and fractional revivals. What is interesting about this case is that we will not only note that they exist, but find a way to characterize how long the smooth revivals live before dephasing.

As in the previous chapter, we are primarily interested in distributions of the weighting constants P_n centered around some mean value, \bar{n} , with spread Δn , such that $1 \ll \Delta n \ll \bar{n}$. In that case we

¹Our treatment of quantum beats is based largely on that in [Leichtle et al., 1996b, Leichtle et al., 1996a].

²For more on the experimental aspects of quantum beats, see [Silverman, 1995].

can define $k = n - \bar{n}$, perform a Taylor expansion of $E(n)$ around \bar{n} , and define

$$\frac{2\pi}{T_j} = \frac{E^{(j)}(\bar{n})}{j!}, \quad (3.2)$$

we can write $f(t)$ as follows:

$$f(t) = \exp(iE_{\bar{n}}t) \sum_k P_{\bar{n}+k} \exp 2\pi i \left(\frac{t}{T_1}k + \frac{t}{T_2}k^2 + \frac{t}{T_3}k^3 + \dots \right). \quad (3.3)$$

Henceforth, we will ignore the leading phase term, as it has no impact on $\|f(t)\|^2$. Note that the T_j are not necessarily positive. When we interpret them as characteristic time scales, we will consider their absolute values, but allowing them to be negative simplifies our formalism. We will use this form of $f(t)$ for the remainder of this chapter. For examples of two different sets of P_n , one a Gaussian distribution and the other a “top hat” distribution, both with $T_2/T_1 = 200$, see Figures 3.1 and 3.2. These specific examples will be treated in detail later in this chapter.

3.1 The Early Phase of the Evolution

The convenience introduced by considering P_n instead of $\psi_n(x)$ is that we can use the Poisson summation formula to recast the sum in Equation 3.3 as a sum of time-separated signals. The Poisson summation formula³ is

$$\sum_{l=-\infty}^{\infty} \int_{-\infty}^{\infty} g(k) \exp(-2\pi i l k) dk = \sum_{k=-\infty}^{\infty} g_k, \quad (3.4)$$

where $g(k)$ is an arbitrary continuous function such that $g(k) = g_k$. Using this formula, we can rewrite Equation 3.3 as

$$f(t) = \sum_{l=-\infty}^{\infty} \int_{-\infty}^{\infty} dk P(k) \exp 2\pi i \left(\left(\frac{t}{T_1} - l \right) k + \frac{t}{T_2}k^2 + \frac{t}{T_3}k^3 + \dots \right), \quad (3.5)$$

³For a derivation, see [Courant and Hilbert, 1953].

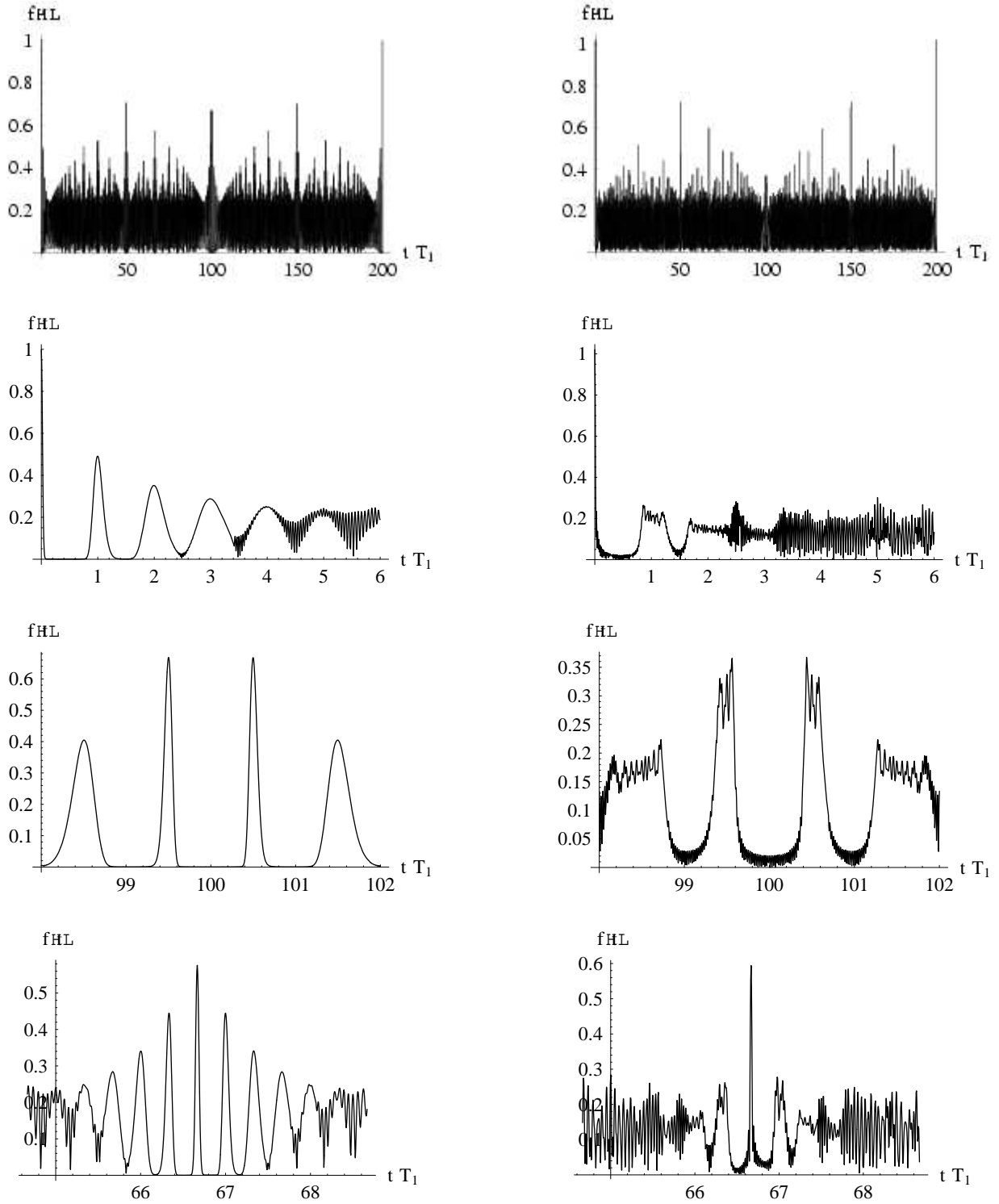


Figure 3.1: A Gaussian distribution of the P_k , with $T_2/T_1 = 200$ and $\sigma_n = 8$. In the plot of the early evolution, by Equation 3.29 dephasing should occur at $t \approx 3.125T_1$.

Figure 3.2: A Gaussian distribution of the P_k , with $T_2/T_1 = 200$ and $N = 8$. In the plot of the early evolution, by Equation 3.53 dephasing should occur at $t \approx 3.125T_1$.

where we interpret each integral term as a signal in time. Of course, this only constitutes a useful simplification when each integral term has a width in time that is less than the distance from its neighboring signals. Also note that our choice of $P(k)$ has a significant impact on the tractability of the integral. Fortunately, the only restriction on $P(k)$ imposed by the Poisson summation formula is that it be continuous and that $P(k) = P_k$.

3.2 Fractional Revivals

It would be surprising if we were not able to combine our use of the Poisson summation formula in the previous section with the fractional revival technique of the previous chapter. As there, we might begin by assuming that it is the influence of T_2 that will dominate most of the behavior beyond the scale of T_1 . Our definition of a fractional revival must change a bit – here we mean the appearance of smooth oscillation at times less than T_2 . To that end, we will start near a time that is an integer multiple of T_1 and also close to a rational fraction of T_2 ,

$$t_{p/q} \equiv lT_1 + \Delta t = \frac{p}{q}T_2 + \epsilon_{p/q}T_1 + \Delta t. \quad (3.6)$$

Note that $|\epsilon_{p/q}| \leq 1/2$. At $t = t_{p/q}$ we can rewrite Equation 3.3 as follows:

$$f(t = t_{p/q}) = \sum_{k=-\infty}^{\infty} P_{\bar{n}+k} \exp 2\pi i \left(\frac{p}{q}k^2 \right) \exp 2\pi i \left(\frac{\Delta t}{T_1}k + \left(\epsilon_{p/q} + \frac{\Delta t}{T_1} \right) \frac{T_1}{T_2}k^2 + \left(l + \frac{\Delta t}{T_1} \right) \frac{T_1}{T_3}k^3 + \dots \right). \quad (3.7)$$

If we define

$$w_k = \exp 2\pi i \left(\frac{p}{q}k^2 \right), \quad (3.8)$$

$$s_k(\Delta t) = P_{\bar{n}+k} \exp 2\pi i \left(\frac{\Delta t}{T_1}k + \left(\epsilon_{p/q} + \frac{\Delta t}{T_1} \right) \frac{T_1}{T_2}k^2 + \left(l + \frac{\Delta t}{T_1} \right) \frac{T_1}{T_3}k^3 + \dots \right), \quad (3.9)$$

we can rewrite the sum as

$$f(t = t_{p/q}) = \sum_{k=-\infty}^{\infty} w_k s_k(\Delta t). \quad (3.10)$$

Note that w_k , the weighting factor, is related to ϕ_k (Equation 2.16) from the previous chapter – $w_k = \exp(-2\pi i) \phi_k$. In analogy with that, we define

$$j = \begin{cases} q, & q \text{ contains one or zero powers of } 2, \\ \frac{q}{2}, & q \text{ contains more than one power of } 2, \end{cases}$$

the minimum period for w_k , just as we defined l , the minimum period of ϕ_k in Section 2.3. Since we can write $w_k = w_{k+mj}$, where m is an integer, we can use the formula

$$\sum_{k=-\infty}^{\infty} a_k = \sum_{r=0}^{j-1} \sum_{m=-\infty}^{\infty} a_{r+mj} \quad (3.11)$$

to simplify the sum in Equation 3.10. The periodicity of w_k lets us extract the weighting factor, and rewrite Equation 3.10 as

$$f(t = t_{p/q}) = \sum_{r=0}^{j-1} w_r \sum_{m=-\infty}^{\infty} s_{r+mj}(\Delta t). \quad (3.12)$$

This is a form to which we can apply the Poisson summation formula,

$$f(t = t_{p/q}) = \sum_{r=0}^{j-1} w_r \sum_{k=-\infty}^{\infty} \int_{-\infty}^{\infty} s(r + mj, \Delta t) \exp(-2\pi imk) dm, \quad (3.13)$$

where $s(r + mj, \Delta t)$ is, again, a continuous extension of $s_{r+mj}(\Delta t)$ ⁴. This is still not so simple a form as we might like, so we introduce a change of variables, $x = r + mj$, and finally complete our

⁴We just applied the Poisson summation formula to a sum of functions instead of a simple sum. Fortunately, we can think of each Δt as indexing a separate sum, and thus what we have done is a shorthand for applying the Poisson summation formula to a large (uncountably infinite) number of different sums.

serious manipulations,

$$f(t = t_{p/q}) = \frac{1}{j} \sum_{r=0}^{j-1} w_r \sum_{k=-\infty}^{\infty} \exp\left(2\pi i \frac{r}{j} k\right) \int_{-\infty}^{\infty} s(x, \Delta t) \exp\left(-2\pi i \frac{x}{j} k\right) dx. \quad (3.14)$$

We may, of course, rearrange some of these terms in order to make this equation look like more of an improvement over Equation 3.7. We may group all of the time-independent terms together into one new weighting coefficient,

$$W_k = \frac{1}{j} \sum_{r=0}^{j-1} \exp 2\pi i \left(r \frac{2p}{q} + r \frac{k}{j} \right), \quad (3.15)$$

and a time-dependent term,

$$S_k(\Delta t) = \int_{-\infty}^{\infty} dx P(\bar{n} + x) \exp 2\pi i \left(\left(\frac{\Delta t}{T_1} - \frac{k}{j} \right) x + \left(\epsilon_{p/q} + \frac{\Delta t}{T_1} \right) \frac{T_1}{T_2} x^2 + \left(l + \frac{\Delta t}{T_1} \right) \frac{T_1}{T_3} x^3 + \dots \right), \quad (3.16)$$

and arrive at our final form for this sum,

$$f(t = t_{p/q}) = \sum_{k=-\infty}^{\infty} W_k S_k(\Delta t). \quad (3.17)$$

The form of $S_k(\Delta t)$ should evoke the integral in Equation 3.5. In fact, it arises by making the substitutions

$$\left(\frac{t}{T_1} - l \right) \rightarrow \left(\frac{\Delta t}{T_1} - \frac{k}{j} \right), \quad (3.18)$$

$$\frac{t}{T_2} \rightarrow \left(\epsilon_{p/q} + \frac{\Delta t}{T_1} \right) \frac{T_1}{T_2}, \quad (3.19)$$

$$\frac{t}{T_j} \rightarrow \left(l + \frac{\Delta t}{T_1} \right) \frac{T_1}{T_j}, \quad j \geq 3. \quad (3.20)$$

Where the original solutions are centered on $t/T_1 = -l$, the fractional revivals are centered on $\Delta t/T_1 = k/q$, and the T_2 and T_j terms are shifted relative to the T_1 term, though, due to the

hierarchy $|T_1| \ll |T_2| \ll |T_3| \ll \dots$, the shifting should be small. Because of this, the fractional revivals should look very much like the early evolution, further justifying our calling them “Fractional revivals.” That one is able to arrive at the equations for the fractional revivals just by making substitutions, without doing any new integrals, is quite a computational nicety. Finally, note that though each S_k constitutes a fractional revival, as in the previous section these fractional revivals are only distinguishable when they don’t overlap significantly.

3.3 A Special Case: The Gaussian Distribution

The integral that will be used heavily in this subsection is

$$\int_{-\infty}^{\infty} e^{-ax^2+bx} = \sqrt{\frac{\pi}{a}} e^{b^2/4a}, \operatorname{Re}\{a\} > 0. \quad (3.21)$$

We will define $P(x)$ to be

$$P(x) = \frac{1}{\sqrt{2\pi\Delta n^2}} \exp\left[-\frac{(x - \bar{n})^2}{2\Delta n^2}\right], \quad (3.22)$$

a Gaussian distribution of P_n . In order to simplify the integrals, we will assume⁵ $T_j = \infty$, for $j \geq 3$.

⁵For a treatment of a Gaussian distribution of coefficients with non-infinite time scales T_1 , T_2 , and T_3 , see [Leichtle et al., 1996b]. The solutions are in terms of Airy functions, and while the results are quite interesting, plenty of interesting results come from an case with just two time scales.

3.3.1 Early Evolution

We are able to evaluate the integral in Equation 3.5, since it is a product of two Gaussian functions:

$$\begin{aligned}
&= \int_{-\infty}^{\infty} dk \frac{1}{\sqrt{2\pi\Delta n^2}} \exp\left(-\frac{k^2}{2\Delta n^2}\right) \exp 2\pi i \left(\left(\frac{t}{T_1} - l\right) k + \frac{t}{T_2} k^2 \right) \\
&= \int_{-\infty}^{\infty} dk \frac{1}{\sqrt{2\pi\Delta n^2}} \exp\left(2\pi i \left(\frac{t}{T_1} - l\right) k - \left(-2\pi i \frac{t}{T_2} + \frac{1}{2\Delta n^2}\right) k^2\right) \\
&= \frac{1}{\sqrt{2\pi\Delta n^2}} \sqrt{\frac{\pi}{-2\pi i \frac{t}{T_2} + \frac{1}{2\Delta n^2}}} \exp\left(\frac{-4\pi^2 \left(\frac{t}{T_1} - l\right)^2}{4 \left(-2\pi i \frac{t}{T_2} + \frac{1}{2\Delta n^2}\right)}\right) \\
&= \frac{1}{\sqrt{1 - 4\pi i \Delta n^2 t / T_2}} \exp\left(-\frac{2\pi^2 \Delta n^2}{1 - 4\pi i \Delta n^2 t / T_2} \left(\frac{t}{T_1} - l\right)^2\right). \tag{3.23}
\end{aligned}$$

We can write this as a product of two Gaussians, one of real and one of imaginary argument, by rewriting the argument of the exponential,

$$\frac{a}{1 - bi} = \frac{a}{1 + b^2} + \frac{abi}{1 + b^2}, \tag{3.24}$$

$$\frac{2\pi^2 \Delta n^2}{1 - 4\pi i \Delta n^2 t / T_2} = \frac{2\pi^2 \Delta n^2}{1 + 16\pi^2 \Delta n^4 t^2 / T_2^2} + i \frac{8\pi^3 \Delta n^4 t / T_2}{1 + 16\pi^2 \Delta n^4 t^2 / T_2^2}, \tag{3.25}$$

defining the (time-dependent) widths,

$$\sigma_r^2(t) = \frac{1}{2} \left[\frac{1}{2\pi^2 \Delta n^2} + 8\Delta n^2 \frac{t^2}{T_2^2} \right], \tag{3.26}$$

$$\sigma_i^2(t) = \frac{1}{2} \left[\frac{1}{8\pi^3 \Delta n^4 t / T_2} + \frac{2}{\pi} \frac{t}{T_2} \right], \tag{3.27}$$

and writing $f(t)$ as

$$f(t) = \sum_{l=-\infty}^{\infty} \frac{1}{\sqrt{1 - 4\pi i \Delta n^2 t / T_2}} \exp\left(-\frac{\left(\frac{t}{T_1} - l\right)^2}{2\sigma_r^2(t)}\right) \exp\left(-i \frac{\left(\frac{t}{T_1} - l\right)^2}{2\sigma_i^2(t)}\right). \tag{3.28}$$

Equation 3.28 holds exactly so long as our assumptions are true (note that a Gaussian distribu-

tion of coefficients is always going to be truncated, so long as there is some minimum n , introducing an error function). $f(t)$ consists of a sum of Gaussian packets separated in time and expanding as time increases, multiplied by a phase factor. These Gaussian packets begin to interfere significantly when their widths becomes comparable to their separation, $2 \times 2\sigma_r(t) = 1$,

$$\begin{aligned} \frac{4}{\sqrt{2}} \sqrt{\frac{1}{2\pi^2\Delta n^2} + 8\Delta n^2 \frac{t^2}{T_2^2}} &= 1, \\ 16\Delta n^2 \left(\frac{t}{T_2}\right)^2 &= \frac{1}{4} - \frac{1}{\pi^2\Delta n^2}, \\ \frac{t}{T_2} &= \frac{1}{8\Delta n} \sqrt{1 - \frac{1}{\pi^2\Delta n^2}}, \\ \frac{t}{T_1} &= \frac{T_2}{T_1} \frac{1}{8\Delta n} \sqrt{1 - \frac{1}{\pi^2\Delta n^2}} \\ &\approx \frac{T_2}{T_1} \frac{1}{8\Delta n} \left(1 - \frac{1}{2\pi^2\Delta n^2}\right), \quad \Delta n \gg 1. \end{aligned} \quad (3.29)$$

Notice that this dephasing time is roughly proportional to $1/\Delta n$. If we then write $\Delta t \approx T_2/2\Delta n$ as the uncertainty of this state in time and consider

$$\begin{aligned} \Delta E &= \hbar(E(\bar{n} + \Delta n) - E(\bar{n} = \Delta n)) \\ &= 2\pi\hbar \left(\frac{2\Delta n}{T_1} + \frac{4\bar{n}\Delta n}{T_2}\right) \\ &= 4\pi\hbar\Delta n \left(\frac{1}{T_1} + \frac{2\bar{n}}{T_2}\right), \end{aligned} \quad (3.30)$$

as the uncertainty in energy, than we have recovered an uncertainty relation,

$$\Delta t \Delta E \approx 2\pi\hbar \left(\frac{T_2}{T_1} + 2\bar{n}\right). \quad (3.31)$$

I believe this uncertainty relation to be related to one of the same form that appears in textbooks on quantum mechanics⁶. There, Δt is the time it takes for the expectation value of an observable to change by one standard deviation – a measure of how long it takes a system to change substantially.

⁶See, for example, [Griffiths, 1995, 112-114].

What we are measuring here is not stated in terms of observables, but it is a way of measuring how long it takes our signal to undergo an important, qualitative change.

3.3.2 Fractional Revivals

Fortunately, to consider the case of fractional revivals we need only apply Equations 3.18 and 3.19 to Equations 3.28. Doing this, we find

$$f(t = t_{p/q}) = \sum_{k=-\infty}^{\infty} \frac{1}{\sqrt{1 - 4\pi i \Delta n^2 (\epsilon_{p/q} + \Delta t/T_1) T_1/T_2}} \exp\left(-\frac{\left(\frac{\Delta t}{T_1} + \frac{k}{q}\right)^2}{2\sigma_r^2(t = t_{p/q})}\right) \exp\left(-i\frac{\left(\frac{\Delta t}{T_1} + \frac{k}{q}\right)^2}{2\sigma_i^2(t = t_{p/q})}\right), \quad (3.32)$$

$$\sigma_r^2(t = t_{p/q}) = \frac{1}{2} \left[\frac{1}{2\pi^2 \Delta n^2} + 8\Delta n^2 \left(\epsilon_{p/q} + \frac{\Delta t}{T_1}\right)^2 \left(\frac{T_1}{T_2}\right)^2 \right], \quad (3.33)$$

$$\sigma_i^2(t = t_{p/q}) = \frac{1}{2} \left[\frac{1}{8\pi^3 \Delta n^4 (\epsilon_{p/q} + \Delta t/T_1) T_1/T_2} + \frac{2}{\pi} \left(\epsilon_{p/q} + \frac{\Delta t}{T_1}\right) \frac{T_1}{T_2} \right]. \quad (3.34)$$

Unfortunately, we cannot simply apply Equations 3.18 and 3.19 to Equation 3.29, as the separation between peaks is no longer 1, but $1/q$. Instead, we require $2\sigma_r(t = t_{p/q}) = 1/q$. This leads us to the dephasing condition

$$\begin{aligned} \frac{4}{\sqrt{2}} \sqrt{\frac{1}{2\pi^2 \Delta n^2} + 8\Delta n^2 \left(\epsilon_{p/q} + \frac{\Delta t}{T_1}\right)^2 \left(\frac{T_1}{T_2}\right)^2} &= \frac{1}{q}, \\ 16\Delta n^2 \left(\epsilon_{p/q} + \frac{\Delta t}{T_1}\right)^2 \left(\frac{T_1}{T_2}\right)^2 &= \frac{1}{4q^2} - \frac{1}{\pi^2 \Delta n^2}, \\ \left(\epsilon_{p/q} + \frac{\Delta t}{T_1}\right) &= \frac{T_2}{T_1} \frac{1}{8\Delta n} \sqrt{\frac{1}{q^2} - \frac{1}{\pi^2 \Delta n^2}}, \\ \left(\epsilon_{p/q} + \frac{\Delta t}{T_1}\right) &= \frac{T_2}{T_1} \frac{1}{8\Delta n} \frac{1}{q} \sqrt{1 - \frac{1}{q^2 \pi^2 \Delta n^2}} \\ &\approx \frac{1}{q} \frac{T_2}{T_1} \frac{1}{8\Delta n} \left(1 - \frac{1}{2q^2 \pi^2 \Delta n^2}\right), \quad \Delta n \gg 1 \end{aligned} \quad (3.35)$$

Comparing Equations 3.35 and 3.29, we see that for a fractional revival at $t = t_{p/q}$, we will see almost exactly the same time evolution we saw at early times, contracted by a factor of $1/q$. Refer

again to Figure 3.1 if you don't believe us.

3.4 A Special Case: The Flat Distribution

The integral that will be used heavily in this subsection is

$$\int_{-N}^N e^{-ax^2+bx} = \sqrt{\frac{\pi}{a}} e^{b^2/4a} \frac{1}{2} \left(\operatorname{Erf} \left(\frac{2aN+b}{2\sqrt{a}} \right) + \operatorname{Erf} \left(\frac{2aN-b}{2\sqrt{a}} \right) \right), \quad (3.36)$$

the integral of a Gaussian truncated at $\pm N$, where $\operatorname{Erf}(x)$ is the error function⁷, defined as

$$\operatorname{Erf}(x) = \frac{2}{\sqrt{\pi}} \int_0^x e^{-t^2} dt. \quad (3.37)$$

Erf is odd, $\operatorname{Erf}(0) = 0$, $\operatorname{Erf}(\infty) = 1$. From this we can conclude that as N becomes large, the error function term should go to one. We will define the “top hat” distribution $P(x)$ to be

$$P(x) = \begin{cases} 1, & |x - \bar{n}| \leq N, \\ 0, & |x - \bar{n}| > N, \end{cases} \quad (3.38)$$

which describes a flat distribution of width $2N$ centered around \bar{n} . This is an interesting case for several reasons. First, it is the other obviously integrable case, along with the Gaussian case. It is also an example of a distribution with sharply limited extent in n -space, unlike the Gaussian. It is, in a sense, the most un-Gaussian of localized distributions. Finally, if we study $\lim_{N \rightarrow \infty}$, we can gain some understanding of an “ultra-localized” spatial distribution⁸ As in the previous example, in order to simplify the integrals, we will assume $T_j = \infty$ for $j \geq 3$.

⁷For a discussion of Erf , see either the more traditional [Abramowitz and Stegun, 1965] or the hip and modern [Wolfram, 2002].

⁸Remember that our ultimate goal is to relate these results to quantum mechanics problems, and we would expect that a broad distribution in energy-space would correspond to a narrow distribution in position-space. While in doing this problem we will break a great number of mathematical rules. $P(x)$ is not continuous, as the Poisson summation formula demands, which casts a shadow on any analysis that we do. Studying $\lim_{N \rightarrow \infty}$ has us implicitly using negative energies, and if we were to try this in quantum mechanics we would have a non-normalizable state that probably wasn't differentiable, and thus not even a solution to the Schrödinger Equation. All the same, we can hope through this savagery to gain some physical insight.

3.4.1 Early Evolution

As above, we are able to evaluate the integral in Equation 3.5, since it is a truncated Gaussian function:

$$\begin{aligned}
 f(t) &= \int_{-N}^N dk \frac{1}{\sqrt{2\pi N^2}} \exp\left(\left(\frac{t}{T_1} - l\right) 2\pi i k + 2\pi i \frac{t}{T_2} k^2\right) \\
 &= \frac{1}{\sqrt{2\pi N^2}} \sqrt{\frac{\pi}{-2\pi i t/T_2}} \exp\left(-\frac{4\pi^2 \left(\frac{t}{T_1} - l\right)^2}{8\pi i t/T_2}\right) \frac{1}{2} \left(\text{Erf}\left(\frac{-4\pi i \frac{t}{T_2} N + 2\pi i \left(\frac{t}{T_1} - l\right)}{2\sqrt{-2\pi i t/T_2}}\right) \right. \\
 &\quad \left. + \text{Erf}\left(\frac{-4\pi i \frac{t}{T_2} N - 2\pi i \left(\frac{t}{T_1} - l\right)}{2\sqrt{-2\pi i t/T_2}}\right) \right). \tag{3.39}
 \end{aligned}$$

We can simplify the arguments of the error functions,

$$\frac{-4\pi i \frac{t}{T_2} N \pm 2\pi i \left(\frac{t}{T_1} - l\right)}{2\sqrt{-2\pi i t/T_2}} = \frac{1}{2} \sqrt{-i} \sqrt{2\pi \frac{t}{T_2}} \left(2N \mp \frac{T_2}{t} \left(\frac{t}{T_1} - l\right)\right), \tag{3.40}$$

and recognize the sum of error functions, which shape the wave packet for a given l , as being of the form

$$\text{Erf}(\alpha\phi(A - x)) + \text{Erf}(\alpha\phi(A + x)), \tag{3.41}$$

where

$$\phi = \sqrt{-i}, \tag{3.42}$$

$$\alpha = \sqrt{\frac{\pi}{2} \frac{t}{T_2}}, \tag{3.43}$$

$$A = 2N, \tag{3.44}$$

$$x = \frac{T_2}{t} \left(\frac{t}{T_1} - l\right). \tag{3.45}$$

From here, it is helpful to first examine Figures 3.3 and 3.4 , plots of $\text{Erf}(\phi x)$ and $\text{Erf}(-\phi x)$. These suggest that if we are to study the modulus of Equation 3.39, that we would do well to consider the

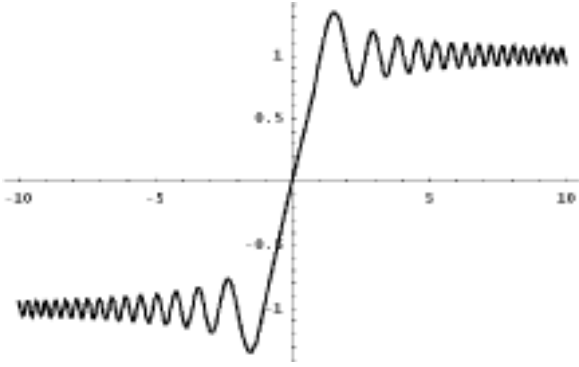


Figure 3.3: $\text{Re}\{\text{Erf}(\phi x)\}$, $x \in [-10, 10]$.

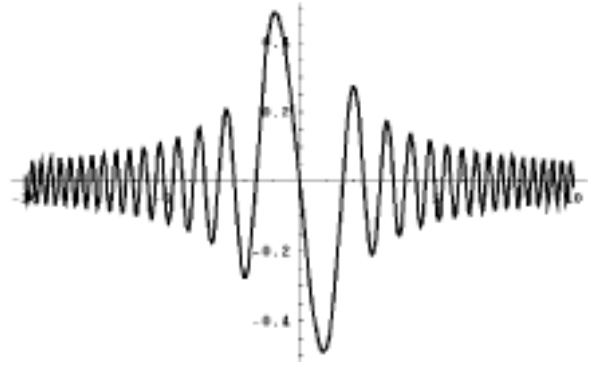


Figure 3.4: $\text{Im}\{\text{Erf}(\phi x)\}$, $x \in [-10, 10]$.

real and imaginary parts separately. Doing this, we find

$$\begin{aligned}
 \|\text{Erf}(\alpha\phi(A-x)) + \text{Erf}(\alpha\phi(A+x))\|^2 &= \|\text{Erf}(\alpha\phi(A-x))\|^2 + \|\text{Erf}(\alpha\phi(A+x))\|^2 + \\
 &\quad \text{Erf}(\alpha\phi(A-x))\text{Erf}(\alpha\phi^*(A+x)) + \\
 &\quad \text{Erf}(\alpha\phi^*(A-x))\text{Erf}(\alpha\phi(A+x)) \\
 &= \text{Re}\{\text{Erf}(\alpha\phi(A-x))\}^2 + \text{Im}\{\text{Erf}(\alpha\phi(A-x))\}^2 + \\
 &\quad \text{Re}\{\text{Erf}(\alpha\phi(A+x))\}^2 + \text{Im}\{\text{Erf}(\alpha\phi(A+x))\}^2 + \\
 &\quad 2\text{Re}\{\text{Erf}(\alpha\phi(A-x))\}\text{Re}\{\text{Erf}(\alpha\phi(A+x))\} + \\
 &\quad 2\text{Im}\{\text{Erf}(\alpha\phi(A-x))\}\text{Im}\{\text{Erf}(\alpha\phi(A+x))\}.
 \end{aligned}$$

Here we see that, roughly, $\text{Im}\{\text{Erf}(\phi x)\} = 0 + \epsilon(x)$ and $\text{Re}\{\text{Erf}(\phi x)\} = \text{Sign}(x)(1 + \epsilon'(x))$, where $\epsilon(x)$ and $\epsilon'(x)$ are functions that describe the oscillations. Obviously, both $\epsilon(x)$ and $\epsilon'(x)$ decrease as $|x|$ increases. We can then observe that in the region $x < -A$, the contribution from Re terms

in Equation 3.46 are roughly

$$\begin{aligned}
&= \operatorname{Re} \{\operatorname{Erf}(\alpha\phi(A+x))\}^2 + \operatorname{Re} \{\operatorname{Erf}(\alpha\phi(A-x))\}^2 + 2\operatorname{Re} \{\operatorname{Erf}(\alpha\phi(A-x))\} \operatorname{Re} \{\operatorname{Erf}(\alpha\phi(A+x))\} \\
&= (-1 - \epsilon'(x))^2 + (-1)^2 + 2(-1 - \epsilon'(x)) \\
&\approx 1 + 2\epsilon'(x) + 1 - 2 - 2\epsilon'(x) = 0.
\end{aligned} \tag{3.47}$$

The same calculation can be performed for the $\operatorname{Im}\{\}$ terms, and for $x > A$, thus demonstrating that anything interesting that happens in the modulus of this sum of error functions happens between $-A$ and A . Although our characterization of the width of the pulse described by Equation 3.46 is not so transparent as the standard deviation of a Gaussian curve, we can say that we have described a pulse are centered on $x = 0$, with width $2A$.

Analysis of Equation 3.40, the argument in our particular problem, is also not so simple as it was in the case of the Gaussian distribution. First, let us find the edges of our pulse – times that satisfy $x = -A$ and $x = A$, respectively, in Equation 3.46. We will define these two times, t_2 and t_1 , as follows:

$$\frac{t_1}{T_1} \equiv \frac{l}{1 + 2N\frac{T_1}{T_2}}, \tag{3.48}$$

$$\frac{t_2}{T_1} \equiv \frac{l}{1 - 2N\frac{T_1}{T_2}}. \tag{3.49}$$

Clearly, $t_2 - t_1$ defines the width of the pulse, and $(t_1 + t_2)/2$ defines its center. If we define the spacing between pulses as the distance between their centers, then that spacing is

$$\frac{1}{2} \left(\frac{1}{1 + 2N\frac{T_1}{T_2}} + \frac{1}{1 - 2N\frac{T_1}{T_2}} \right) = \frac{1}{1 - \left(2N\frac{T_1}{T_2}\right)^2}. \tag{3.50}$$

We are now looking for the spacing for the the value of l for which the spacing between packets equals the width of a packet, the value of l for which we think the packets will overlap enough to

interfere substantially:

$$\begin{aligned}
 2 \left(\frac{t_2}{T_1} - \frac{t_1}{T_1} \right) &= \frac{1}{1 - \left(2N \frac{T_1}{T_2} \right)^2}, \\
 \frac{8NlT_1/T_2}{1 - \left(2N \frac{T_1}{T_2} \right)^2} &= \frac{1}{1 - \left(2N \frac{T_1}{T_2} \right)^2}, \\
 l &= \frac{T_2}{T_1} \frac{1}{8N}.
 \end{aligned} \tag{3.51}$$

We convert this into a time by multiplying it by T_1 ,

$$t = T_1 l = \frac{T_2}{8N}, \tag{3.52}$$

and finally write

$$\frac{t}{T_2} = \frac{1}{8N}. \tag{3.53}$$

As in the Gaussian case, the time after which our signal dephases depends on $1/N$. Looking for an uncertainty relation, we have $\Delta t = T_2/2N$ and, as in the Gaussian example, $\Delta E = 4\pi\hbar N (1/T_1 + 2\bar{n}/T_2)$ and we recover an uncertainty relation,

$$\Delta t \Delta E = 2\pi\hbar \left(\frac{T_2}{T_1} + 2\bar{n} \right), \tag{3.54}$$

the same relation that we found in the Gaussian example, though in that case the result was not exact. If we refer to Figure 3.2, though, we find that our dephasing time doesn't seem to fall in the right place. I submit that the noise between the $t = 2T_1$ and the $t = 3T_1$ pulses is not the dephasing that we were looking for, as it is followed by the discernible top of the $t = 3T_1$ pulse.

3.4.2 Fractional Revivals

Applying Equations 3.18 and 3.19 to the results of the previous section, we find our signal to be

$$f(t = t_{p/q}) = \frac{1}{2\sqrt{2\pi N^2}} \sqrt{\frac{\pi}{-2\pi i(\epsilon_{p/q} + \Delta t/T_1)(T_1/T_2)}} \exp\left(-\frac{4\pi^2\left(\frac{\Delta t}{T_1} - \frac{k}{q}\right)^2}{8\pi i(\epsilon_{p/q} + \Delta t/T_1)(T_1/T_2)}\right) \times \quad (3.55)$$

$$\left(\operatorname{Erf}\left(\frac{-4\pi i(\epsilon_{p/q} + \Delta t/T_1)(T_1/T_2)N - 2\pi i\left(\frac{\Delta t}{T_1} - \frac{k}{q}\right)}{2\sqrt{-2\pi i(\epsilon_{p/q} + \Delta t/T_1)(T_1/T_2)}}\right) \right.$$

$$\left. \operatorname{Erf}\left(\frac{-4\pi i(\epsilon_{p/q} + \Delta t/T_1)(T_1/T_2)N + 2\pi i\left(\frac{\Delta t}{T_1} - \frac{k}{q}\right)}{2\sqrt{-2\pi i(\epsilon_{p/q} + \Delta t/T_1)(T_1/T_2)}}\right) \right),$$

which could be simplified. More interesting is, of course, our dephasing condition. The method that we use to find this is the same one that we used in the previous section.

We started with our simplification of the arguments of the error functions, in Equation 3.40, which we will convert,

$$\frac{1}{2}\sqrt{-2\pi i\frac{t}{T_2}}\left(2N \mp \frac{T_2}{t}\left(\frac{t}{T_1} - l\right)\right) \rightarrow \frac{1}{2}\sqrt{-2\pi i\left(\epsilon_{p/q} + \frac{\Delta t}{T_1}\right)\left(\frac{T_1}{T_2}\right)}\left(2N \mp \frac{\frac{\Delta t}{T_1} - \frac{k}{q}}{(\epsilon_{p/q} + \Delta t/T_1)(T_1/T_2)}\right). \quad (3.56)$$

We now look for the roots of this,

$$\frac{1}{(\epsilon_{p/q} + \Delta t/T_1)(T_1/T_2)}\left(\frac{\Delta t}{T_1} - \frac{k}{q}\right) = \pm 2N,$$

$$\frac{\Delta t}{T_1} - \frac{k}{q} = \pm 2N\frac{T_1}{T_2}\left(\epsilon_{p/q} + \frac{\Delta t}{T_1}\right),$$

$$\frac{\Delta t}{T_1}\left(1 \mp 2N\frac{T_1}{T_2}\right) = \frac{k}{q} \pm 2N\frac{T_1}{T_2}\epsilon_{p/q},$$

$$\frac{\Delta t}{T_1} = \frac{\frac{k}{q} \pm 2N\frac{T_1}{T_2}\epsilon_{p/q}}{1 \mp 2N\frac{T_1}{T_2}}, \quad (3.57)$$

and label those roots,

$$\frac{\Delta t_1}{T_1} \equiv \frac{\frac{k}{q} + 2N\frac{T_1}{T_2}\epsilon_{p/q}}{1 - 2N\frac{T_1}{T_2}}, \quad (3.58)$$

$$\frac{\Delta t_2}{T_1} \equiv \frac{\frac{k}{q} - 2N\frac{T_1}{T_2}\epsilon_{p/q}}{1 + 2N\frac{T_1}{T_2}}. \quad (3.59)$$

We're now interested in the width of the pulses,

$$\begin{aligned} \left(\frac{\Delta t_1}{T_1} - \frac{\Delta t_2}{T_1} \right) &= \frac{4N\frac{T_1}{T_2}\epsilon_{p/q} + 4N\frac{T_1}{T_2}\frac{k}{q}}{1 - \left(2N\frac{T_1}{T_2}\right)^2} \\ &= \left(\epsilon_{p/q} + \frac{k}{q} \right) \frac{4N\frac{T_1}{T_2}}{1 - \left(2N\frac{T_1}{T_2}\right)^2}, \end{aligned} \quad (3.60)$$

and the spacing between pulses,

$$\frac{1}{2} \left(\frac{1/q}{1 - 2N\frac{T_1}{T_2}} + \frac{1/q}{1 + 2N\frac{T_1}{T_2}} \right) = \frac{1}{q} \frac{1}{1 - \left(2N\frac{T_1}{T_2}\right)^2}. \quad (3.61)$$

We now find when these are equal,

$$\begin{aligned} 2 \left(\epsilon_{p/q} + \frac{k}{q} \right) \frac{4N\frac{T_1}{T_2}}{1 + \left(2N\frac{T_1}{T_2}\right)^2} &= \frac{1}{q} \frac{1}{1 + \left(2N\frac{T_1}{T_2}\right)^2}, \\ \frac{k}{q} &= \frac{T_2}{T_1} \frac{1}{8N} \frac{1}{q} - \epsilon_{p/q}, \end{aligned} \quad (3.62)$$

and see that for fractional revivals as well, the dephasing time is proportional to $1/N$, and decreases as q increases. Again, we see that the behavior near $t = 0$ will appear again, squished by a factor of $1/q$. In fact, this result corresponds as closely to the one in the Gaussian case (Equation 3.35) as our results for the early evolution did. It would appear that the principle difference between the signals generated by these two dissimilar distributions is that the sharp edges of the top-hat distribution create the same kind of high-frequency “ringing” that we would expect from a truncated

sum of harmonic functions.

3.5 Summary

In this chapter we studied a zero-dimensional system that exhibits “quantum beats,” which is both of experimental interest, and, due to its low dimensionality, is a nice system on which to introduce our Poisson summation formula technique. The principal advantage of this technique is that it allows us to quantify the dephasing of an initial wavepacket. We have seen that, for quantum beats, fractional revivals are related to the early evolution of the packet by the simple substitution of a few terms. In the specific examples that we have considered, a Gaussian distribution of weighting coefficients and a “top hat” distribution, we have discovered nearly-identical dephasing conditions. If Δn is the “spread” of the weighting coefficients, then the initial dephasing time goes as $T_2/8\Delta n$, and the dephasing time for a fractional revival at $t = t_{p/q}$ goes as $T_2/8\Delta nq$, and the fractional revival has the same number of “clean” oscillations as there were oscillations near $t = 0$. That these distributions are so different from each other suggests that many well-localized distributions of coefficients should demonstrate similar behavior.

Chapter 4

The Connection Between Beats and Carpets

One shortcoming of the previous chapter is that it describes a zero-dimensional problem which, while interesting, lacks the spatial features that we would like to consider. The main advantage of the quantum beats approach is that it allows us to not only identify pseudoclassical behavior at full and fractional revivals, but also to associate a particular lifetime with those revivals. In both of the examples that we considered we found that the lifetime of the revivals was proportional to $1/\Delta n$, the spread of the wavepacket in energy-space, but two cases hardly exhausts all of the possible localized wavepackets. Although we could think of revivals of a spatial wavefunction as revivals of each point, we know that even a simple distribution of weighting coefficients will become complicated when it is combined with the eigenfunctions evaluated at a particular point. How, then, can we connect this approach with quantum carpets?

4.1 Abuse of the Poisson Summation Formula

So long as we can come up with a continuous extension of a set of functions $f_m(\vec{x})$, we have a generalization of the Poisson summation formula,

$$\sum_{m=-\infty}^{\infty} f_m(\vec{x}) = \sum_{l=-\infty}^{\infty} \int_{-\infty}^{\infty} f(m, \vec{x}) e^{-2\pi i m l} dm. \quad (4.1)$$

Not all sets of functions will have an obvious continuous extension, but we can find extensions in cases where our eigenfunctions are continuous functions of m and \vec{x} . So long as we are able to make this extension, it is easy to apply the formulae derived in the previous parts of this chapter to an n -dimensional problem, by making the substitution $P_k \rightarrow c_k \psi_k(\vec{x})$. This is our crucial observation in this section, but its merit will not be clear until we have examined at least one case.

4.2 A Special Case: Gaussian Weighting Coefficients in the Infinite Square Well

The attentive reader will have noticed that the integral hiding in Equation 4.1 is a bit intimidating. In order to be sure that it's even worth thinking about, we'll do it for the simplest case I can think of – the infinite square well. We'll take advantage of two characteristics of solutions to the square well: the eigenfunctions are just sine waves, easily converted into exponentials, and the spectrum is quadratic in the quantum number, meaning that a Taylor expansion of the spectrum is exact and gives just two time-scales. All of our integrals will reduce to Gaussian integrals, which we can do.

4.2.1 Algebra

For this case, we will write our wavefunction as

$$\Psi(x, t) = \sqrt{\frac{2}{L}} \sum_{k=-\infty}^{\infty} c_{\bar{n}+k} \sin\left(\frac{\bar{n}+k}{L}\pi x\right) \exp\left[-2\pi i \left(\frac{t}{T_1}k + \frac{t}{T_2}k^2\right)\right], \quad (4.2)$$

where we have set the weighting coefficients to be

$$c_{\bar{n}+k} = \frac{1}{\sqrt{2\pi\Delta\bar{n}^2}} e^{-\frac{k^2}{2\Delta\bar{n}^2}}, \quad (4.3)$$

and defined

$$T_1 = \frac{2\pi}{2\pi^2\bar{n}/L^2} = \frac{L^2}{\pi\bar{n}}, \quad (4.4)$$

$$T_2 = \frac{2\pi}{\pi^2/L^2} = \frac{2L^2}{\pi}, \quad (4.5)$$

$$\frac{T_1}{T_2} = \frac{1}{2\bar{n}}. \quad (4.6)$$

What follows is a godawful bit of algebra, and in order to make it easier to follow (and ensure that I get it right), I'm going to temporarily replace all of these compound constants with simpler ones. I'm also going to ignore multiplication by leading constants – don't worry, I'll put it all back in later. If you're not interested in this, you won't have missed much by skipping directly to Equation 4.27. We will define

$$\xi = \frac{x}{L}, \quad (4.7)$$

$$\tau = \frac{t}{T_1}, \quad (4.8)$$

and use these, along with Equation 4.6 to define the following:

$$a = \frac{1}{2\Delta n^2}, \quad (4.9)$$

$$b = \frac{\bar{n}\pi}{L}x = \frac{1}{2}\frac{T_2}{T_1}\pi\xi, \quad (4.10)$$

$$c = \frac{\pi}{L}x = \pi\xi, \quad (4.11)$$

$$d = 2\pi\frac{t}{T_1} = 2\pi\tau, \quad (4.12)$$

$$f = 2\pi\frac{t}{T_2} = 2\pi\frac{T_1}{T_2}\tau, \quad (4.13)$$

$$g = 2\pi l. \quad (4.14)$$

Note that these are all real quantities. Having defined these, we can rewrite our wavefunction as

$$\Psi(x, t) = \sqrt{\frac{2}{L}} \sum_{k=-\infty}^{\infty} \sqrt{\frac{a}{\pi}} \exp(-ak^2) \sin(b + ck) \exp -i (dk + fk^2). \quad (4.15)$$

We now rewrite the sine term as a sum of exponentials,

$$\Psi(x, t) = \frac{1}{2i} \sqrt{\frac{2}{L}} \sum_{k=-\infty}^{\infty} \sqrt{\frac{a}{\pi}} \exp(-ak^2) (\exp i(b + ck) - \exp -i(b + ck)) \exp i(-dk - fk^2), \quad (4.16)$$

combine the exponentials,

$$\Psi(x, t) = \frac{1}{2i} \sqrt{\frac{2}{L}} \sum_{k=-\infty}^{\infty} \sqrt{\frac{a}{\pi}} (\exp (bi + i(c - d)k - (a + if)k^2) - \exp (-bi - i(c + d)k - (a + if)k^2)), \quad (4.17)$$

apply the Poisson summation formula,

$$\Psi(x, t) = \frac{1}{2i} \sqrt{\frac{2}{L}} \sqrt{\frac{a}{\pi}} \sum_{l=-\infty}^{\infty} \int_{-\infty}^{\infty} dk (\exp (bi + i(c - d - g)k - (a + if)k^2) - \exp (-bi - i(c + d + g)k - (a + if)k^2)), \quad (4.18)$$

and do the integration, using the formula $\int_{-\infty}^{\infty} dk \exp(-\alpha x^2 + \beta x) = \sqrt{\pi/\alpha} \exp(\beta^2/4\alpha)$:

$$\Psi(x, t) = \frac{1}{2i} \sqrt{\frac{2}{L}} \sqrt{\frac{a}{\pi}} \sum_{l=-\infty}^{\infty} \sqrt{\frac{\pi}{a+if}} \left(\exp\left(bi - \frac{(c-(d+g))^2}{4(a+if)}\right) - \exp\left(-bi - \frac{(c+(d+g))^2}{4(a+if)}\right) \right). \quad (4.19)$$

We have, in a sense, solved the problem now, but we have gained little unless we can understand this result in a simpler way than we understood the original expression. So long as the terms of the sum are localized in their own regions of spacetime¹, and the region defined by one value of l does not overlap significantly with the region defined by another value of l , we can make the substantial simplification of studying just one term in the sum to understand a particular region. There are, however, some algebraic simplifications that we will make first.

We perform the square in the exponentials,

$$\Psi(x, t) = \frac{1}{2i} \sqrt{\frac{2}{L}} \sqrt{\frac{a}{\pi}} \sum_{l=-\infty}^{\infty} \sqrt{\frac{\pi}{a+if}} \left(\exp\left(bi - \frac{(c^2+(d+g)^2-2c(d+g))}{4(a+if)}\right) - \exp\left(-bi - \frac{(c^2+(d+g)^2+2c(d+g))}{4(a+if)}\right) \right). \quad (4.20)$$

We then turn the difference of exponentials into a product of a sine function and another exponential,

$$\Psi(x, t) = \sqrt{\frac{2}{L}} \sqrt{\frac{a}{\pi}} \sum_{l=-\infty}^{\infty} \sqrt{\frac{\pi}{a+if}} \exp\left(-\frac{(c^2+(d+g)^2)}{4(a+if)}\right) \sin\left(b + \frac{2c(d+g)}{4i(a+if)}\right). \quad (4.21)$$

From here, we would do well to write the arguments of the exponential and the sine in the form $x + iy$,

$$\Psi(x, t) = \sqrt{\frac{2}{L}} \sqrt{\frac{a}{\pi}} \sum_{l=-\infty}^{\infty} \sqrt{\frac{\pi}{a+if}} \exp\left(-\frac{(c^2+(d+g)^2)}{4(a^2+f^2)}(a-if)\right) \sin\left(b + \frac{2c(d+g)}{4(a^2+f^2)}(-f-ia)\right). \quad (4.22)$$

Now, we will consider $\|\Psi(x, t)\|^2$, making the assumption that we can ignore interference between

¹This isn't obvious, but it is something we can hope for, as the Poisson summation formula works kind of like a Fourier transform.

terms in the sum. While this is not obviously true, this whole business is worthless if it isn't. Don't worry, we'll check this assumption at the end, just to be sure. One of the advantages of doing this is that we can use the formula $\|\sin(x + iy)\|^2 = (1/2)(\cosh(2y) - \cos(2x))$. Doing all of this, we find

$$\|\Psi(x, t)\|^2 = \frac{a}{L\sqrt{a^2 + f^2}} \sum_{l=-\infty}^{\infty} \exp - \left(a \frac{c^2 + (d+g)^2}{2(a^2 + f^2)} \right) \left(\cosh \left(a \frac{2c(d+g)}{2(a^2 + f^2)} \right) - \cos 2 \left(b - f \frac{2c(d+g)}{4(a^2 + f^2)} \right) \right). \quad (4.23)$$

Looking at this, we may notice that the adding the argument of the cosh to the argument of the exponential would complete the square. Fortunately, we may write the cosh in terms of exponentials, giving us

$$\|\Psi(x, t)\|^2 = \frac{a}{L\sqrt{a^2 + f^2}} \sum_{l=-\infty}^{\infty} \left(\left(\exp - \left(a \frac{(c+(d+g))^2}{2(a^2+f^2)} \right) + \exp - \left(a \frac{(c-(d+g))^2}{2(a^2+f^2)} \right) \right) \times \right. \quad (4.24) \\ \left. \left(1 - \frac{\cos \left(2b - f \frac{c(d+g)}{a^2+f^2} \right)}{\cosh \left(a \frac{c(d+g)}{a^2+f^2} \right)} \right) \right).$$

This is the simplest form of this equation that I have found. Noticing the ubiquity of $a^2 + f^2$, we define

$$\sigma^2(\tau) = a^2 + f^2 = \left(\frac{1}{2\Delta n^2} \right)^2 + \left(2\pi \frac{t}{T_2} \right)^2, \quad (4.25)$$

then fill in our various constants to arrive at the following,

$$\|\Psi(x, t)\|^2 = \frac{1/2\Delta n^2}{L\sigma(\tau)} \sum_{l=-\infty}^{\infty} \left(\exp - \left(\frac{1}{2\Delta n^2} \frac{(\pi\xi + (2\pi\tau + 2\pi l))^2}{2\sigma^2(\tau)} \right) + \right. \quad (4.26) \\ \left. \exp - \left(\frac{1}{2\Delta n^2} \frac{(\pi\xi - (2\pi\tau + 2\pi l))^2}{2\sigma^2(\tau)} \right) \right) \times \\ \left(1 - \frac{\cos \left(\frac{T_2}{T_1} \pi\xi - 2\pi \frac{T_1}{T_2} \tau \frac{\pi\xi(2\pi\tau + 2\pi l)}{\sigma^2(\tau)} \right)}{\cosh \left(\frac{1}{2\Delta n^2} \frac{\pi\xi(2\pi\tau + 2\pi l)}{\sigma^2(\tau)} \right)} \right) \\ = \frac{1}{2L\Delta n^2\sigma(\tau)} \sum_{l=-\infty}^{\infty} \left(\left(\exp - \left(\frac{\pi^2}{2\Delta n^2} \frac{(\xi - 2(\tau+l))^2}{2\sigma^2(\tau)} \right) + \exp - \left(\frac{\pi^2}{2\Delta n^2} \frac{(\xi + 2(\tau+l))^2}{2\sigma^2(\tau)} \right) \right) \right. \quad (4.27) \\ \left. \left(1 - \cos \pi \left(\frac{T_2}{T_1} \xi - 4\pi^2 \frac{T_1}{T_2} \tau \frac{\xi(\tau+l)}{\sigma^2(\tau)} \right) \operatorname{sech} \left(\frac{\pi^2}{\Delta n^2} \frac{\xi(\tau+l)}{\sigma^2(\tau)} \right) \right) \right).$$

4.2.2 Interpretation

We are now prepared to discuss Equation 4.27. Most of the structure is provided by the two travelling Gaussians, which both originate at $\xi = 0$, $\tau = -l$, then separate and travel along straight lines to $\xi = 1$, $\tau = -l \pm 1/2$. This both provides a pleasing picture of a packet completing one classical oscillation in one classical period (T_1), and tells us that if the packets in two neighboring terms have $\sigma(\tau) < 1/2$, those terms will have negligible interference². All of this is modulated by the final, oscillating term, which provides “interference without cross terms.” Note that because $|\cos| \leq 1$ and $\text{sech} \leq 1$, the oscillating term will always fall between zero and two, and makes a secondary contribution. We have left things in terms of the ratio T_1/T_2 as a reminder that a principal difference between classical and quantum dynamics is that a classical system would have only one time scale (T_1), while a quantum system may have more – in this case, two. Note that by Equation 4.6, the limit as $\bar{n} \rightarrow \infty$ is identical to the limit $T_1/T_2 \rightarrow 0$, and that this fixes the widths of the travelling Gaussians above. That is, in the classical limit our packet does not spread.

When we are not in the classical limit, three things prevent our travelling Gaussians from behaving classically. First, there is a damping term in front of the Gaussians, though this isn’t difficult to interpret – it enforces conservation of probability. Second, their widths *do* increase, and when those widths become larger than the width of the well we would expect significant interference between, for example, the l th term and the $(l + 1)$ th term. Finally, there is the oscillatory term. In the cosine term, the $(T_2/T_1)\xi$ term guarantees rapid oscillations, and the other term serves to curve the paths along which the $\cos \times \text{sech}$ term is constant. The oscillation of the cosine term is modulated by the slowly-varying sech term. Although there is no conventional characteristic width defined for this function, as there is for a Gaussian distribution, it is clear that when the argument of the sech function becomes large, our Gaussians will look fairly smooth, and the argument of sech is on the order of one, the unsuppressed cosine will produce oscillatory interference-like effects.

We can see all of this by plotting several terms from the sum in Equation 4.27 and comparing it to a similar region of the full expansion of Equation 4.2 (see Figure 4.1). One thing that you

²Of course, the “no overlap” assumption is going to break down in some interval near $\xi = 1$.

won't notice unless you plot some of these yourself is that where Equation 4.27 is valid, it is more computationally efficient – there are no cross terms to calculate. For an example of this, see Figure 4.2.

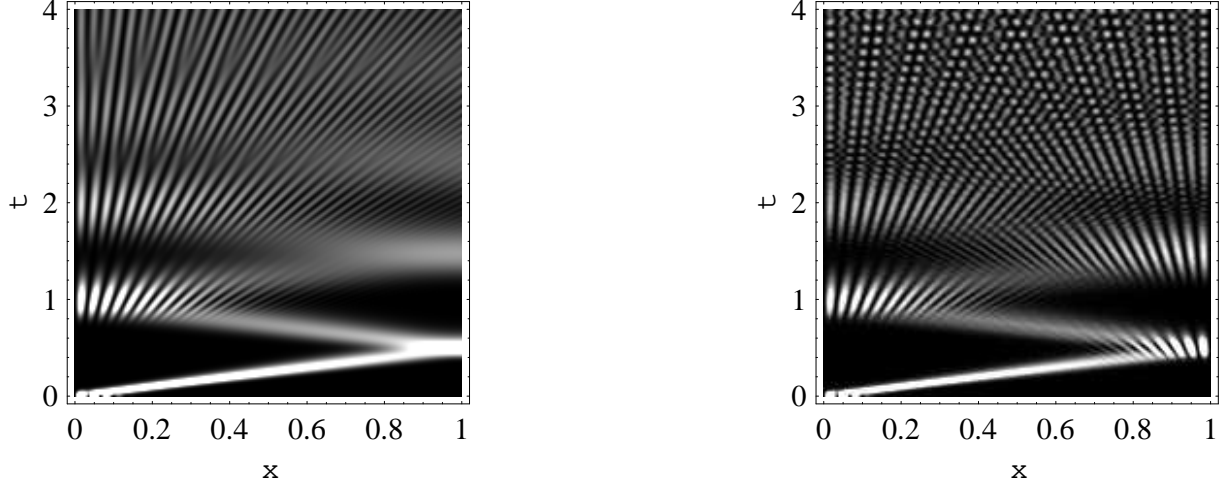
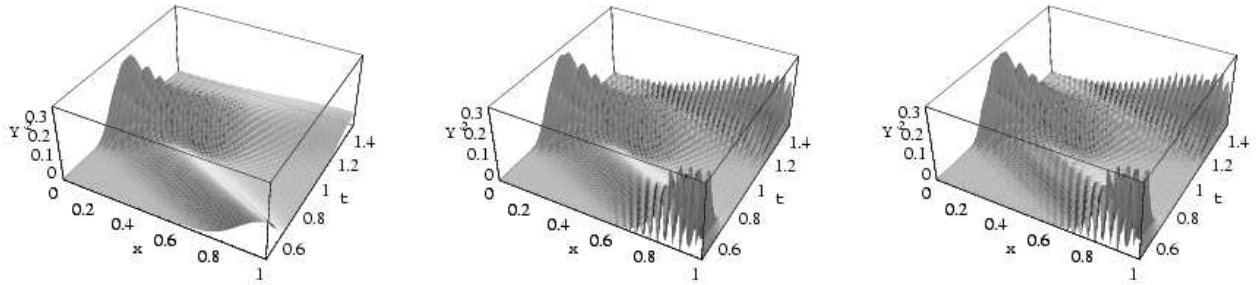


Figure 4.1: These density plots show a solution of the infinite square well in the region $\tau \in [0, 4]$, $\xi \in [0, 1]$ for $\Delta n = 5$, $\bar{n} = 30$. On the left are the five relevant terms from Equation 4.27, on the right are the middle 10 terms of the sum in Equation 4.2.

4.2.3 A Quick Look at Sech

One function that appears in Equation 4.27 and may be unfamiliar is sech, the hyperbolic secant. Defined as $\text{sech}(y) = 1/\cosh(y)$, it has a peak at $y = 0$, $\text{sech}(y) = 1$, and $\lim_{|y| \rightarrow \infty} = 0$. In fact, it looks rather like a Gaussian wavepacket. How much? Consider Figure 4.3, which suggests that near $y = 0$ the functions can be given similar characteristic widths. For example, choosing a constant $\alpha = \text{ArcSech}(1/e^2) \approx 2.69$ gives us $\exp(-y^2/2\sigma^2) \approx \text{sech}(\alpha y/2\sigma)$, which becomes exact at $y = \pm 2\sigma$. We can generalize this result still further. Suppose we want $\exp(-y^2/2\sigma^2) = \text{sech}(\alpha y/A\sigma)$ at $y = \pm A\sigma$. We will first find that

$$\exp\left(-\frac{(A\sigma)^2}{2\sigma^2}\right) = \exp(-A^2/2). \quad (4.28)$$



6.188s

207.891s

106.047s

Figure 4.2: All of these show the region $\tau \in [0.5, 1.5]$, $\xi \in [0, 1]$ for $\Delta n = 5$, $\bar{n} = 30$, and the time it took *Mathematica* to plot them. On the left is the $l = -1$ term from Equation 4.27, the middle figure contains the middle 20 terms of the sum in Equation 4.2, and at right is a plot of the middle 10 terms from that same Equation.

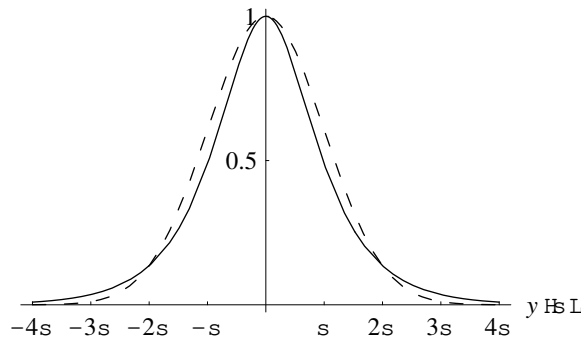


Figure 4.3: A plot of $\exp\left(-\frac{y^2}{2\sigma^2}\right)$ (dashed) and $\operatorname{sech}\left(\alpha\frac{y}{2\sigma}\right)$ (solid), $-5\sigma \leq y \leq 5\sigma$. The constant $\alpha = \operatorname{arcsech}\left(\frac{1}{2}\right) \approx 2.69$ is chosen so that the two functions are equal at $y = \pm 2\sigma$.

Comparing this with

$$\begin{aligned}\operatorname{sech}\left(\alpha\frac{A\sigma}{A\sigma}\right) &= \operatorname{sech}(\alpha) \\ &= \exp(-A^2/2),\end{aligned}\tag{4.29}$$

we can see that $\alpha(A)$ must be

$$\alpha(A) = \operatorname{arcsech}\left(e^{-A^2/2}\right).\tag{4.30}$$

Note that the domain of $\operatorname{arcsech}$ is $(0,1]$, the same as the range of $\exp(-x^2)$, so $\alpha(A)$ is defined for all real values of A .

Now, our final step of generalization. Suppose we want to find the condition for

$$\exp\left(-\frac{(y-a)^2}{2\sigma_a^2}\right) = \operatorname{sech}\left(\alpha(A)\frac{y-b}{A\sigma_b}\right)\tag{4.31}$$

to hold at $y = \pm_1 A\sigma_a = \pm_2 A\sigma_b$. This equation is clearly satisfied when

$$(y-a) = \pm_1 A\sigma_a,\tag{4.32}$$

$$(y-b) = \pm_2 A\sigma_b,\tag{4.33}$$

where I have used subscripts on the \pm symbols to indicate their independence. It would be unfortunate if our goal was just to find the intersections of two given functions. That is, if we were searching for the solutions of

$$\exp\left(-\frac{(y-a)^2}{2\sigma_a^2}\right) = \operatorname{sech}\left(\frac{y-b}{\sigma_b}\right),\tag{4.34}$$

where we were unwilling to vary any of the parameters. This will quickly lead us to the transcendental equation

$$A\sigma_a + a = \alpha(A)\sigma_b + b,\tag{4.35}$$

which I don't care to solve. However, if we fix A and choose to solve for one of the other variables, we will have an ordinary algebraic equation with perhaps one unsightly transcendental number floating around. Since we are only concerned with equality at a point, we can even allow a , b , σ_a , and σ_b to be functions. In that case, the result in Equations 4.32 and 4.33 are quite useful. They let us figure out what parameter values to use to get these functions to intersect at, say, one standard deviation from their centers, which is exactly the what we need to do in order to find dephasing times.

4.2.4 Dephasing of the Wavepacket

If we recall the previous chapter, the advantage of this sort of analysis of the wavefunction is that it allows us to quantitatively understand when the wavefunction makes the transition from semiclassical motion to characteristically quantum mechanical motion. We could assume that this happens when the sech term overlaps the Gaussian closer to $\tau = 0$ – then we need only decide what constitutes substantial overlap. Let us suppose that it occurs when some particular number of “standard deviations” of the sech function reach a particular number of standard deviations of the travelling Gaussian (we'll not specify on which side of its center), so that the functions are equal at that point. This condition may be more clear when written like Equations 4.32 and 4.33:

$$\left(\tau + \left(l + \frac{\xi}{2} \right) \right) = \pm A \sigma_{\text{exp}}(\tau), \quad (4.36)$$

$$(\tau + l) = -A \sigma_{\text{sech}}(\tau), \quad (4.37)$$

where we have defined $\sigma_{\text{sech}}(\tau)$ and $\sigma_{\text{exp}}(\tau)$ in terms of $\sigma(\tau)$, from Equation 4.25,

$$\sigma_{\text{sech}}(\tau) = \frac{\alpha(A)}{A\xi} \left(\frac{\Delta n}{\pi} \sigma(\tau) \right)^2, \quad (4.38)$$

$$\sigma_{\text{exp}}(\tau) = \frac{\Delta n}{\pi} \sigma(\tau), \quad (4.39)$$

$$\sigma^2(\tau) = \left(\frac{1}{2\Delta n^2} \right)^2 + \left(2\pi \frac{T_1}{T_2} \tau \right)^2. \quad (4.40)$$

Note that the \pm in Equation 4.36 allows us to consider intersection on either side of the center of the Gaussian, while the fixed sign in Equation 4.37 indicates our choice to consider only the region between $\tau = -l$ and $\tau = 0$. Keep in mind that what we are doing is, in spirit, exactly what we did in the previous chapter. We have used the Poisson summation formula to turn a sum of functions over all space into a sum of localized functions, figured out how to characterize their widths, and now we are preparing to find out when those widths overlap, in order to discover when interference effects become *really* important to the time-evolution – when our wavepacket has dephased. We will now combine Equations 4.32 and 4.33 to eliminate $\tau + l$ and solve for $\sigma(\tau)$:

$$\begin{aligned} -A\sigma_{\text{sech}}(\tau) + \frac{\xi}{2} &= \pm A\sigma_{\text{exp}}(\tau), \\ -\frac{\alpha(A)}{\xi} \left(\frac{\Delta n}{\pi} \sigma(\tau) \right)^2 + \frac{\xi}{2} &= \pm A \frac{\Delta n}{\pi} \sigma(\tau), \\ -\frac{\alpha(A)}{\xi} \left(\frac{\Delta n}{\pi} \sigma(\tau) \right)^2 \mp A \left(\frac{\Delta n}{\pi} \sigma(\tau) \right) + \frac{\xi}{2} &= 0. \end{aligned} \quad (4.41)$$

We may now use the quadratic equation to solve for $(\Delta n \sigma(\tau)) / \pi$,

$$\begin{aligned} \frac{\Delta n}{\pi} \sigma(\tau) &= \frac{\pm_1 A \pm_2 \sqrt{A^2 + 4 \frac{\alpha(A)}{\xi} \frac{\xi}{2}}}{-2 \frac{\alpha(A)}{\xi}} \\ &= -\frac{A\xi}{2\alpha(A)} \left(\pm_1 1 \pm_2 \sqrt{1 + 2 \frac{\alpha(A)}{A^2}} \right). \end{aligned} \quad (4.42)$$

Since $\alpha(A)$ and A are always positive, we know that the square root term will always be greater than one. We now square this equation, to recover something in terms of $\sigma^2(\tau)$,

$$\left(\frac{\Delta n}{\pi} \right)^2 \sigma^2(\tau) = \left(\frac{A\xi}{2\alpha(A)} \right)^2 \left(1 + \left(1 + 2 \frac{\alpha(A)}{A^2} \right) \pm 2 \sqrt{1 + 2 \frac{\alpha(A)}{A^2}} \right), \quad (4.43)$$

which we can further simplify

$$\sigma^2(\tau) = \frac{1}{2} \left(\frac{\pi A \xi}{\Delta n \alpha(A)} \right)^2 \left(1 + \frac{\alpha(A)}{A^2} \pm \sqrt{1 + 2 \frac{\alpha(A)}{A^2}} \right), \quad (4.44)$$

before inserting Equation 4.25,

$$\begin{aligned} \left(\frac{1}{2\Delta n^2}\right)^2 + \left(2\pi\frac{T_1}{T_2}\tau\right)^2 &= \frac{1}{2}\left(\frac{\pi A\xi}{\Delta n\alpha(A)}\right)^2\left(1 + \frac{\alpha(A)}{A^2} \pm \sqrt{1 + 2\frac{\alpha(A)}{A^2}}\right), \\ \tau^2 &= \left(\frac{1}{2\pi}\frac{T_2}{T_1}\right)^2\left(\frac{1}{2}\left(\frac{\pi A\xi}{\Delta n\alpha(A)}\right)^2\left(1 + \frac{\alpha(A)}{A^2} \pm \sqrt{1 + 2\frac{\alpha(A)}{A^2}}\right) - \left(\frac{1}{2\Delta n^2}\right)^2\right), \\ \tau &= \frac{\sqrt{2}}{4\pi\Delta n}\frac{T_2}{T_1}\sqrt{\left(\frac{\pi A\xi}{\alpha(A)}\right)^2\left(1 + \frac{\alpha(A)}{A^2} \pm \sqrt{1 + 2\frac{\alpha(A)}{A^2}}\right) - \frac{1}{2\Delta n^2}} \end{aligned} \quad (4.45)$$

Note that the τ at which dephasing occurs depends (to first order) on $1/\Delta n$, as in all of our other examples. To check that this works, let's compare the lower of the $A = 1$ terms against plots of Equations 4.27 and 4.2 in Figure 4.4. Note that the plots agree quite nicely in the left half

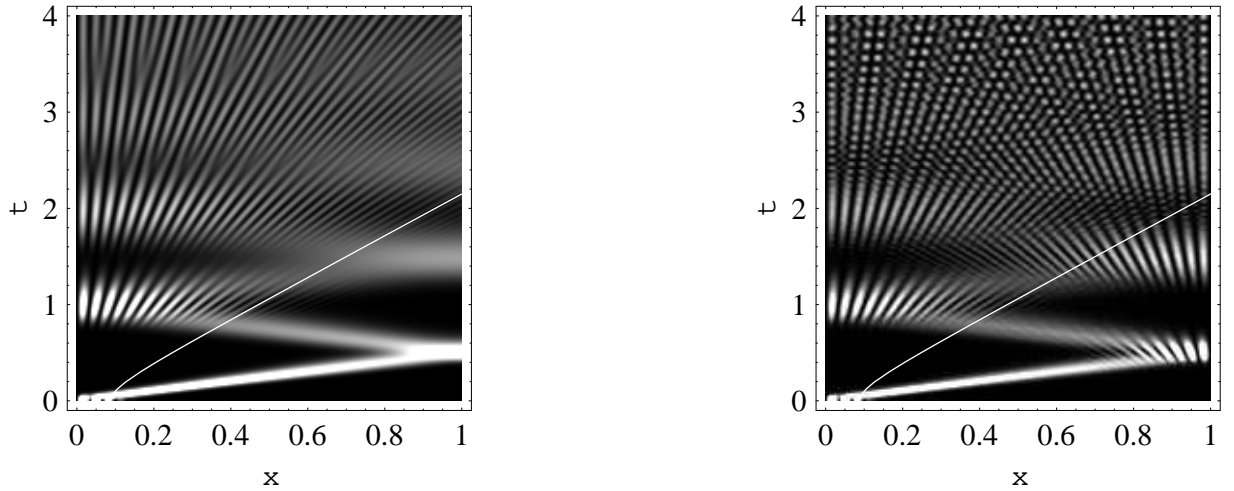


Figure 4.4: These density plots show a solution of the infinite square well in the region $\tau \in [0, 4]$, $\xi \in [0, 1]$ for $\Delta n = 5$, $\bar{n} = 30$, and the white line indicates the lower of the $A = 1$ solutions of Equation 4.45. On the left are the five relevant terms from Equation 4.27, on the right are the middle 10 terms of the sum in Equation 4.2. Note that the ridges in the left plot only appear above the line, and in the right plot that this holds for $\xi < 1/2$ – for $\xi > 1/2$, the interference between terms in Equation 4.27 becomes non-negligible.

of the well, but that where different terms in Equation 4.27 overlap, i.e. near the right wall, our

approximation does not reproduce the appropriate interference effects. Nevertheless, Equation 4.45 does predict where rippling begins in the left side of the well. If we wanted to set different standards for overlap, we would just need to change the value of A . We could also treat fractional revivals in the square well, but the reader should be able to combine the results of Section 3.2 and those of this section to quickly find and study them.

4.3 Solutions in More Complicated Potentials

Obviously, we have little interest in actually doing the integral in Equation 4.1. At the same time, there are many interesting potentials that we might consider which are not the infinite square well – which, indeed, do not even admit solutions in pure exponentials. Our analytical approach to these rogues will be to use the WKB approximation to render much of the information about the wavefunction in convenient exponential form.

4.3.1 The WKB Approximation

The WKB approximation³ is a formalization of the observation that if a wavefunction has sufficient energy that it undergoes rapid oscillations in comparison to the “features” of the potential below it, it looks much like a free particle. It is useful in the same sorts of semiclassical problems where we would expect to find interesting revival and carpet phenomena. Without going into too many details, we define

$$p_n(x) = \sqrt{E_n - V(x)}, \quad (4.46)$$

which will behave rather like a wave number. It is subject to the Bohr-Sommerfeld condition,

$$\int_{x_l}^{x_r} p_n(x) dx = n\pi, \quad (4.47)$$

³For a more complete treatment of the WKB approximation, see [Griffiths, 1995, 274-292]

which enforces quantization of energy. x_l and x_r are, respectively, the left and right classical turning points for a particle of energy E_n . We are then able to write the wavefunction as

$$\psi_n(x) \approx \frac{C_n}{\sqrt{p_n(x)}} \exp\left(i \int^x p_k(x') dx'\right) + \frac{D_n}{\sqrt{p_n(x)}} \exp\left(-i \int^x p_k(x') dx'\right), \quad (4.48)$$

with the understanding that both $\int^x p(x') dx'$ and $1/\sqrt{p_n(x)}$ vary slowly in comparison to $\exp(i \int^x p(x') dx')$. C and D are constants of integration. This approximation of the wavefunction breaks down when E_n is not much greater than $V(x)$, near the classical turning points.

4.3.2 The WKB Approximation and the Poisson Summation Formula

The WKB approximation has not quite solved our problem, having both left that unattractive $1/\sqrt{p_k(x)}$ term in from of our exponentials. We are, however, *en route* to a solution,

$$\begin{aligned} \Psi(x, t) &= \sum_{l=-\infty}^{\infty} \int_{-\infty}^{\infty} c_k \psi_k(x) \exp(-iE_k t) \\ &= \sum_{l=-\infty}^{\infty} \int_{-\infty}^{\infty} dk \left(\frac{c(k)}{\sqrt{p_k(x)}} \exp -i \left(- \int^x p_k(x') dx' + E_k t + 2\pi k l \right) + \right. \\ &\quad \left. \frac{d(k)}{\sqrt{p_k(x)}} \exp -i \left(\int^x p_k(x') dx' + E_k t + 2\pi k l \right) \right), \end{aligned} \quad (4.49)$$

but the remaining integral is still less than inviting. Of course, judicious choice of the c_k and d_k will make matters simpler, but we can do more than that. We now perform a Taylor expansion of $\int^x p_k(x') dx'$, E_k , $c(k)/\sqrt{p_k(x)}$, and $d(k)/\sqrt{p_k(x)}$ around $k = 0$. For the terms that appear in the exponential, we would keep up to order $k^2 - k^3$ if we felt like using Airy functions. Keep as many terms as you like in the expansion of $1/\sqrt{p_k(x)}$. The resulting mess will be some Gaussian integral which will be easy to evaluate in closed form. We should find some sum of exponentials, trigonometric, and hyperbolic functions, including some which we can identify as containing much of the interference information, and find the condition for wavepacket dephasing.

Our solution relies on three successive approximations – the WKB approximation, the application of the Poisson summation formula (which involves an extension of the c_n , d_n beyond $k = -\bar{n}$

to $k = -\infty$ and eventual neglect of cross terms), and a Taylor expansion of the remaining functions – and obviously won't work in all cases. There are doubtless examples which can be integrated that neither bear resemblance to the square well nor require that we resort to these approximations. However, we have here a quantitative way of finding out the lifetime of a wavepacket in an arbitrary potential well.

4.4 Summary

In this chapter we demonstrated that the Poisson summation formula technique, developed on zero-dimensional quantum beats in Chapter 3, can also be applied to problems with more dimensions. We demonstrated this by using the technique to solve the square well, arriving at a very elegant sum of successive travelling Gaussians multiplied by interference terms. From this, we were able to derive a dephasing condition, though instead of finding a simple time we found a function $\tau(\xi)$. What's more, it only works in the left half of the well, due to interference that we had to neglect. Fortunately, we found a $\tau \propto (T_2/T_1)/4\Delta n$ component in the dephasing condition that is strongly reminiscent of our dephasing results from Chapter 3. The case of fractional revivals is left as an exercise for the reader.

Chapter 5

Intermode Traces and Quantum Carpets

5.1 Multimode Interference

The Multimode Interference technique¹ is a devilishly simple way of studying the interference patterns formed by a quantum system. It allows us to understand both the existence of canals and ridges in the carpet and the role that the spectrum and potential play in generating carpets. We will begin by rewriting the probability density as a sum of multimode terms (defined below) instead of eigenfunctions. Starting with a wavefunction,

$$\Psi(x, t) = \sum_{n=1}^{\infty} c_n \psi_n(\vec{x}) e^{-iE_n t}, \quad (5.1)$$

we define a multimode term as

$$\mu_{nm}(x, t) = \frac{1}{2} (d_{nm} \psi_n(x, t) \psi_m^*(x, t) \exp -it (E_n - E_m) + d_{mn} \psi_n^*(x, t) \psi_m(x, t) \exp -it (E_m - E_n)), \quad (5.2)$$

$$d_{nm} = c_n c_m^* = d_{mn}^*, \quad (5.3)$$

¹The first sections of this chapter are based on [Kaplan et al., 2000]. I have tried to make their work more clear and rigorous.

and write the probability density as

$$\|\Psi(x, t)\|^2 = \sum_{n,m=1}^{\infty} \mu_{nm}(x, t). \quad (5.4)$$

This is not, at first glance, a particularly good idea. We have simply grouped the terms in the sum differently and not achieved any obvious simplification. The advantage is that we may simply add multimode terms – they already contain all of the information about how the eigenfunctions interfere. If we can figure out a way to tease that information out of the multimode terms, we will have been successful.

5.2 Characteristic Velocities

As in the previous chapter, we will use the WKB approximation to study semiclassical cases (see Section 4.3.1). Our approximate eigenstates are then

$$\psi_n(x) \approx \frac{C_n}{\sqrt{p_n(x)}} \exp\left(i \int^x p_n(x') dx'\right) + \frac{D_n}{\sqrt{p_n(x)}} \exp\left(-i \int^x p_n(x') dx'\right), \quad (5.5)$$

where C_n and D_n are complex constants of integration, and our approximate multimode terms will be weighted sums of eight intermode terms, which we define as

$$\iota_{nm}(x, t) = \frac{1}{2} d_{nm} \frac{1}{\sqrt{p_n(x) p_m(x)}} \exp \pm_1 i \left(\int^x (\pm_2 p_n(x') \pm_3 p_m(x')) dx' + (E_n - E_m) t \right). \quad (5.6)$$

Since we are interested in lines of constant phase, we differentiate the argument of the exponential and look for its roots,

$$\begin{aligned} \frac{d}{dt} \pm_1 \left(\int^x (\pm_2 p_n(x') \pm_3 p_m(x')) dx' + (E_n - E_m) t \right) &= 0, \\ \frac{dx}{dt} &= \frac{E_n - E_m}{\pm_2 p_n(x) \pm_3 p_m(x)}, \\ v_{nm} = \frac{\Delta\omega}{\Delta k} &= \pm_1 \frac{E_n - E_m}{\sqrt{E_n - V(x)} \pm_2 \sqrt{E_m - V(x)}} \quad (5.7) \end{aligned}$$

Each pair of quantum numbers, (n, m) , gives rise to *four* velocities v_{nm} .

5.3 Characterization of the Velocities

We have written that last equation in terms of $\Delta\omega/\Delta k$ because this will allow us to label some of the velocities as “group” velocities, and others as what I will tentatively call “not group velocities.”

If we have defined $\omega_n = E_n$ and $k_n(x) = p_n(x)$, then we can write

$$\omega_n(k_n, x) = k_n^2 - V(x). \quad (5.8)$$

If we are considering a semiclassical problem, our weighting coefficients must be well centered on some number N with some spread Δn , such that these satisfy the hierarchy $1 \ll \Delta n \ll N$. This allows us to define a group velocity for our packet,

$$v_{gr} = \left. \frac{d\omega_n}{dk_n} \right|_{n=N} = 2k_N, \quad (5.9)$$

which happens to be the classical velocity of a particle in the potential V with energy E_N . If we then consider the velocities from Equation 5.7, writing $E_n = E_N + e_n$ and $E_m = E_N + e_m$, where $e_n, e_m \ll E_N - V(x)$ we can simplify our expression,

$$\begin{aligned} v_{nm} &= \pm_1 \frac{(E_N + e_n) - (E_N + e_m)}{\sqrt{E_N + e_n - V(x)} \pm_2 \sqrt{E_N + e_m - V(x)}} \\ &\approx \pm_1 \frac{e_n - e_m}{\sqrt{E_N - V(x)} \left(\left(1 + \frac{e_n}{2(E_N - V(x))} \right) \pm_2 \left(1 + \frac{e_m}{2(E_N - V(x))} \right) \right)} \\ &\approx \pm_1 2\sqrt{E_N - V(x)} \frac{e_n - e_m}{2(E_N - V(x)) (1 \pm_2 1) + (e_n \pm_2 e_m)} \\ &\approx \begin{cases} \pm_1 2\sqrt{E_N - V(x)} = \pm_1 2k_N(x), & (-2) \\ \pm_1 2\sqrt{E_N - V(x)} \frac{e_n - e_m}{(E_n - V(x)) + (E_m - V(x))} \approx \pm_1 \frac{\omega_n - \omega_m}{k_N(x)}, & (+2). \end{cases} \end{aligned} \quad (5.10)$$

So long as both $e_n, e_m \ll E_N - V(x)$, as they should be in the semiclassical approximation, then half of the velocities contributed by a particular (n, m) will be comparable to the group velocity, v_{gr} , and half will be smaller. It is important to note (in preparation for the next section) that Equation 5.10 is approximate – it will not happen that half our velocity terms will be degenerate.

These velocities describe paths (the “traces” in the chapter title) along which the phase is constant for a given intermode term. That is, given a particular ι_{nm} and a value of x , we can find the trajectory along which that phase does not change, and we can do this for all values of x . Although what we have done may bear a superficial resemblance to the method of stationary phase, it is very different. We could use the method of stationary phase if each intermode term was highly oscillatory except along a particular path – we would then assume that each term only made a significant contribution to the probability density in the immediate vicinity of the path of stationary phase. This is invalid here because, typically, the phase term in Equation 5.6 will change at a rate determined by the $p_n(x)$, which shouldn’t be particularly high. The picture, rather, is of the phase function at $t = 0$ sliding around (and stretching a bit) as time increases.

5.4 Groups of Velocities and Degeneracy²

The result in Equation 5.10 demonstrates that in any problem we will find a range of velocities. Those results are, however, approximate. We will show that some intermode terms have *exactly* the same maximum velocities, and that because of that we can treat them as essentially moving together. We consider this to be a sort of degeneracy – the sort of degeneracy that produces quantum carpets.

²To this point, my exposition has paralleled that of [Kaplan et al., 2000]. Here, however, I must depart, as their treatment of the problem was incorrect. They blithely assert that to discover the traces, we just need to integrate from the classical turning points. A cursory survey of the figures in this thesis should be enough to convince you otherwise.

If we examine the velocities (Equation 5.7) at a point³ where $V(x) = 0$,

$$v_{nm} = \pm_1 \frac{E_n - E_m}{\sqrt{E_n} \pm_2 \sqrt{E_m}}, \quad (5.11)$$

we can factor the numerator,

$$v_{nm} = \pm_1 \frac{(\sqrt{E_n} + \sqrt{E_m})(\sqrt{E_n} - \sqrt{E_m})}{\sqrt{E_n} \pm_2 \sqrt{E_m}}, \quad (5.12)$$

and arrive at an important condition,

$$v_{nm} = \pm_1 \left(\sqrt{E_n} \mp_2 \sqrt{E_m} \right). \quad (5.13)$$

Terms that have the same v_{nm} at $V(x) = 0$ have the same classical period – these are our degenerate terms.

We immediately gain some insight into the role of quadratic spectra in producing quantum carpets. If the spectrum depends on the the quantum number n squared, then we will have many degenerate velocities, while if the spectrum is linear in the quantum number, only traces which involve two perfect squares may be degenerate. This suggests that if we begin with a system like the simple harmonic oscillator, with a spectrum linear in the quantum number, and set to zero all weighting coefficients that are not perfect squares (selecting only states 1,4,9,16,etc.), we can produce a carpet because we have effectively quadratized⁴ the spectrum. For an example of this, see Figure 5.1.

Of course, the production of the characteristic canals and ridges of a quantum carpet depends not only on degenerate velocities existing, but their producing some sort of peak or valley in the

³Remember that if we can't find a point where $V(x) = 0$, we can exploit our ability to change the potential by a constant and create one.

⁴“Effectively quadratize the spectrum” is my shorthand for choosing weighting coefficients such that only terms that have quantum numbers that are perfect squares are contained in the wavefunction. When we do this, we could rewrite the spectrum, eigenfunctions, etc., as if they were governed by a new variable, $m^2 = n$, as if they had quadratic spectra. Of course, we're not changing the spectrum itself, we're changing the wavefunction.

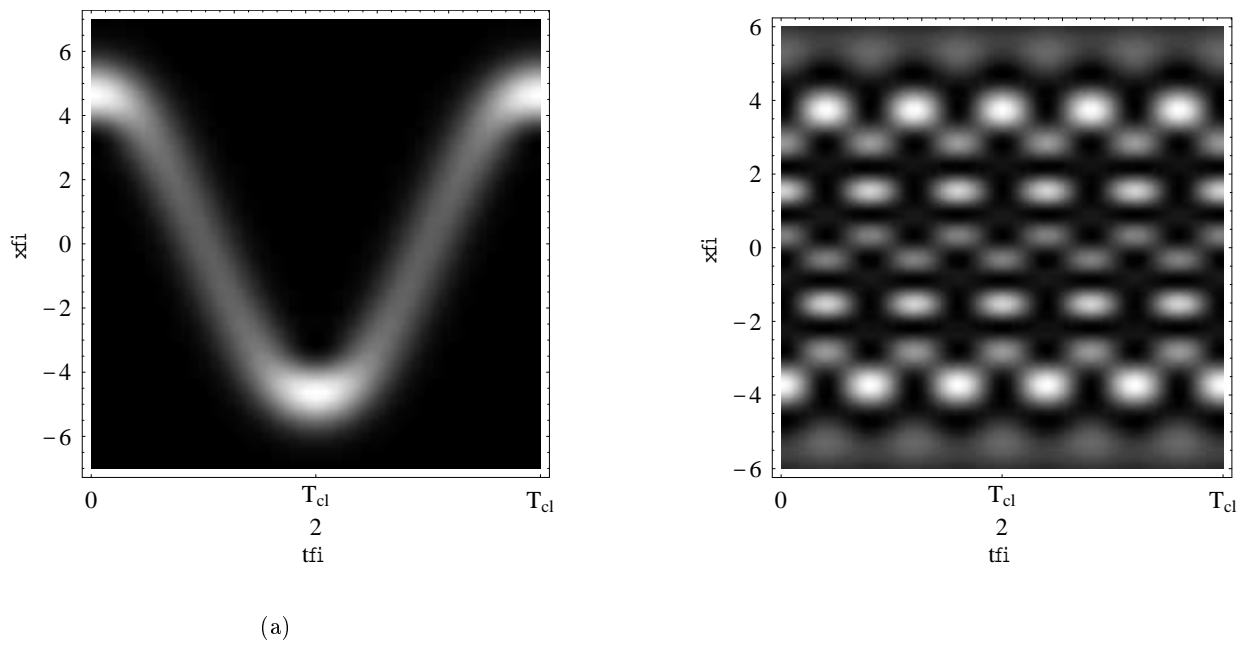


Figure 5.1: Two plots of the simple harmonic oscillator. On the left, the distribution of coefficients is Gaussian, with $\bar{n} = 6$ and $\sigma_n = 2$, while the plot on the right is an even weighting of the perfect squares between 1 and 81.

probability density. Recalling the form for an intermode term,

$$\iota_{nm}(x, t) = \frac{1}{2} d_{nm} \frac{1}{\sqrt{p_n(x) p_m(x)}} \exp \pm_1 i \left(\int^x (\pm_2 p_n(x') \pm_3 p_m(x')) dx' + (E_n - E_m) t \right), \quad (5.14)$$

we can see how a sum of these terms might produce a peak or valley at $t = 0$. First, we ignore the imaginary component of the exponential – since our probability density has been reduced to a sum of these intermode terms, and the probability density must be real, the imaginary terms will ultimately cancel. The sum of intermode terms looks like

$$\sum \iota_{nm}(x, t = 0) = \frac{1}{2} \sum d_{nm} \frac{1}{\sqrt{p_n(x) p_m(x)}} \cos \pm_1 \left(\int^x (\pm_2 p_n(x') \pm_3 p_m(x')) dx' \right), \quad (5.15)$$

or roughly a weighted sum of cosines. Although this hardly constitutes a proof⁵ that peaks and valleys exist, it is not hard to imagine that in many cases we would find them.

A general calculation of the location of the peaks of an intermode trace would be so general as to be useless, and specific examples are likely to be too specific. Instead, we must rest satisfied with the notion that very degenerate velocities will typically have enough terms to form some sort of peak. As we evolve in time, the peak should roughly follow a classical trajectory, experiencing a bit of dispersion. The formula for such a trajectory is

$$t(x) = \int_{x_0}^x \frac{1}{v_{nm}(x')} dx', \quad (5.16)$$

where x_0 is the location of the center of the peak, and v_{nm} is some suitable velocity, perhaps the middlemost of the degenerate velocities. These are the intermode traces that we are interested in. If this all seems a bit hazy, bear in mind that this idea of a “channel” or “ridge” is something we impose on the system, not so easily defined as a local minimum or maximum. We are, in a sense, asking a question of the system that it does not want to answer, and this sort of ambiguity is one of

⁵Of course, proofs are possible here. I suspect, though, that figuring out what one *can* prove will be difficult work in and of itself.

its methods of resistance. Hopefully, future work will uncover a procedure for identifying the most significant traces in the carpet.

5.4.1 A Quick Example

Once again, we will work on the infinite square well. From the wavefunction,

$$\Psi(x, t) = \sqrt{2} \sum c_n \frac{i}{2} \left(e^{+in\pi\xi} - e^{-in\pi\xi} \right) e^{-i\pi^2 n^2 t}, \quad (5.17)$$

we can immediately identify the velocities in question as

$$v_{nm} = \pm_1 \pi (n \pm_2 m). \quad (5.18)$$

We can also find that the wavenumbers k_{nm} will be

$$k_{nm} = \mp_1 \pi (n \mp_2 m), \quad (5.19)$$

so that in any particular velocity bundle there will be a variety of wavenumbers, and we have the hope, at least, of interesting interference – for an example, see Figure 5.2. The most degenerate

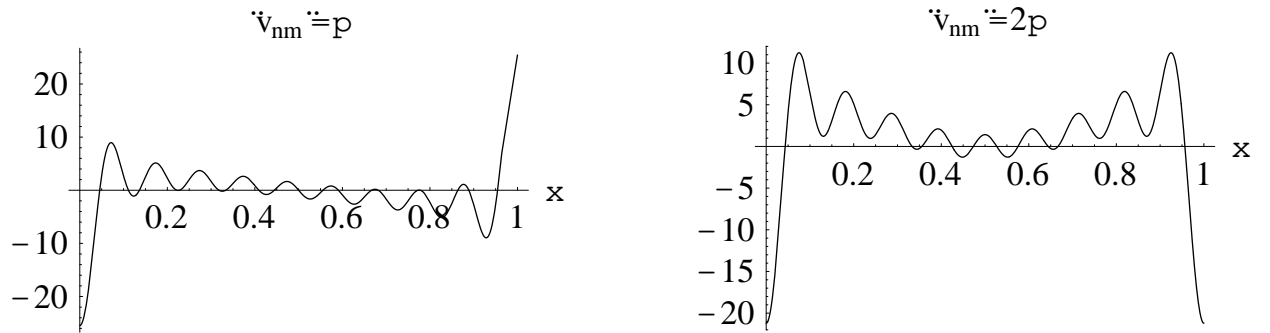


Figure 5.2: The $|v_{nm}| = \pi$ (left) and $|v_{nm}| = 2\pi$ (right) velocity bundles for an even distribution of weighting coefficients between $n = 1$ and $n = 10$ in the infinite square well.

velocity will typically be $v_{nm} = \pm\pi$, and in time $T_R = 2/\pi$, a trajectory with this velocity will cover

a distance of 2 – that is, one full period, so the most prominent traces should have the same period as the revival time. Better still, we can ask what velocity we need to have in order to have a period equal to the classical period, T_{cl} . The condition is

$$\begin{aligned} v_{nm}T_{cl} = v_{nm}\frac{1}{\bar{n}\pi} &= 2 \\ v_{nm} &= 2\pi\bar{n}, \end{aligned} \tag{5.20}$$

which should be satisfied by very few (n, m) pairs. An example of how well our separation of the wavefunction works is shown in Figures 5.3-5.5 .

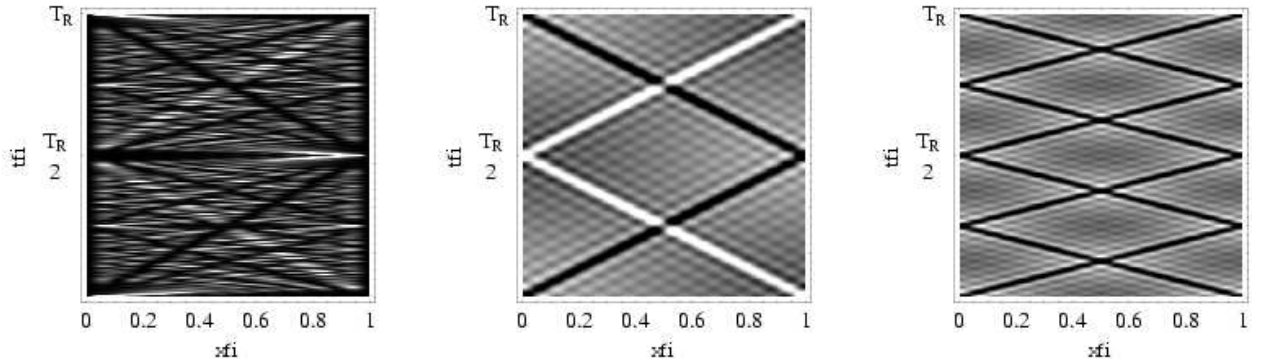


Figure 5.3: The full carpet, coefficients evenly weighted between $n = 1$ and $n = 10$.

Figure 5.4: The $v_{nm} = \pi$ intermode terms. Note that they do, indeed, have a period $T = T_R$.

Figure 5.5: The $v_{nm} = 2\pi$ intermode terms. Note that they have a period $T = T_R/2$.

5.5 Degeneracy and Ψ_{cl}

Recall that Ψ_{cl} is the “classicized” wavefunction from Section 2.3 (see Equation 2.21), and is what governs the spatial distribution and shape of fractional revivals. We have seen that in several cases, Ψ_{cl} looks like the original wavepacket moved along a classical path with a relatively small amount of dispersion, but we can make this understanding more precise by the application of intermode

trace methods.

Observe from the derivation of Equation 5.7 that the $E_n - E_m$ term comes from the time-evolution exponential and the square root terms come from the WKB approximation. If, then, we want to find a similar formula for Ψ_{cl} (see Section 2.3 and Equation 2.21), we replace the $E_n - E_m$ in the numerator with $(2\pi/T_1)(n - m)$. Considering a point where $V(x) = 0$, we find the following velocity degeneracy condition:

$$v_{nm} = \pm_1 \frac{2\pi}{T_1} \frac{n - m}{\sqrt{E_n} \pm_2 \sqrt{E_m}}. \quad (5.21)$$

Unlike Equation 5.13, we have no hope of factoring this in general. We can, however, see what happens in a few obvious cases. If

$$E_n = \alpha^2 n, \quad (5.22)$$

then we quickly find

$$v_{nm} = \pm_1 \frac{2\pi}{T_1 \alpha} \frac{n - m}{\sqrt{n} \pm_2 \sqrt{m}}, \quad (5.23)$$

a degeneracy condition identical to the one we would have found for the harmonic oscillator in the previous section. If, however, we try a spectrum $E_n = \alpha^2 n^2$, we find something far more interesting,

$$v_{nm} = \pm_1 \frac{2\pi}{T_1 \alpha} \frac{n - m}{n \pm_2 m} = \begin{cases} \pm_1 \frac{2\pi}{T_1 \alpha}, (-2), \\ \pm_1 \frac{2\pi}{T_1 \alpha} \frac{n-m}{n+m}, (+2). \end{cases} \quad (5.24)$$

Half of all of the traces are degenerate! Looking at the other half, we want to find two pairs of number, (n, m) and (p, q) that will be degenerate. The conditions are

$$\frac{n - m}{n + m} = \frac{p - q}{p + q}, \quad \begin{array}{l} n + m \neq 0, \quad p + q \neq 0, \\ n \neq p, \quad m \neq q, \end{array} \quad (5.25)$$

which then reduces to

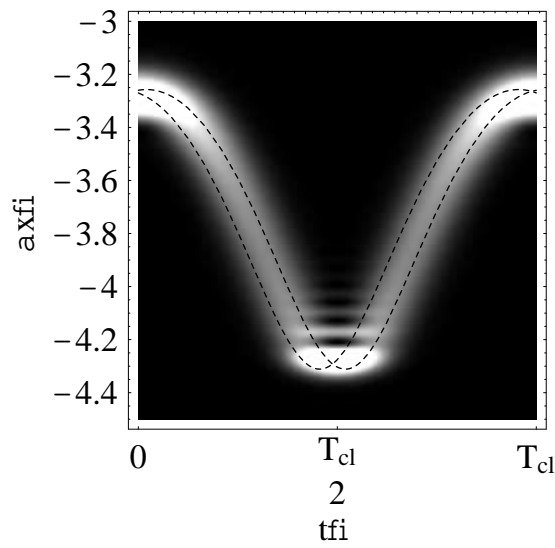
$$\begin{aligned}
 (p+q)(n-m) &= (n+m)(p-q), \\
 qn - mp &= -qn + mp, \\
 \frac{n}{m} &= \frac{p}{q}.
 \end{aligned} \tag{5.26}$$

While this is not a particularly difficult equation to satisfy with all of the integers at our disposal, it is difficult to satisfy when our weighting coefficients are all within some $\Delta n \ll \bar{n}$ of $\bar{n} \gg 1$. The solutions that will lie closest to (n, m) are $(p, q) = 1/2(n, m)$ and $(p, q) = 2(n, m)$. If n and m are in the vicinity of \bar{n} , as they must be in the semiclassical case, that puts p and q near either $\bar{n}/2$ or $2\bar{n}$, both of which would typically be “out of range” of Δn . For the case of a quadratic spectrum, then, we find that half of the velocities are degenerate, and half tend to be non-degenerate. This nicely corresponds with our picture of Ψ_{cl} wavepackets evolving along classical paths (see Figures 2.5 and 2.6).

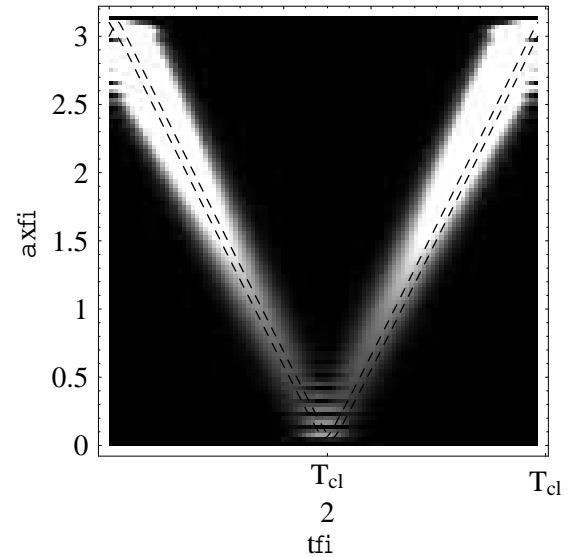
The unfortunate thing about this result for the Ψ_{cl} of a quadratic spectrum is that it is so heavily dependent on the quadraticity of the spectrum. This behavior seems to occur in potentials with non-quadratic spectra as well, as demonstrated in Figure 5.6. My short response to this is that, in the semiclassical limit, their spectra can appear to be no more than quadratic [Nieto and Simmons, 1979]. This leaves low- \bar{n} cases to consider, and completing our understanding of Ψ_{cl} is a possible subject for future work.

5.6 Summary

In this chapter we saw how an analysis of the intermode terms in the probability density of a semiclassical wavefunction can give us insight into the degeneracy conditions which must be met in order to produce a carpet, and into the carpet itself. When those degeneracy conditions are met, we can examine the initial form of certain bundles of velocities and from that find the channels and



(a) The Morse Potential



(b) The Rosen-Morse I Potential

Figure 5.6: Plots of Ψ_{cl} in two potentials, one with a quadratic spectrum and one with a non-quadratic spectrum. On the left is the Morse Potential, with $E_n = A^2 - (A - \alpha n)^2$, and on the right the Rosen-Morse I potential, with $E_n = -A^2 + (A + \alpha n)^2 - (B/(A + \alpha n))^2 + (B/A)^2$. In both cases A , B , and α are independent constants. The black lines overlaying the maxima are classical paths for those potentials with $E = E_{\bar{n}}$. For more on these potentials, see Sections A.2.1 and A.2.6.

ridges of the quantum carpet. For a problem with a spectrum linear in the quantum number it was almost impossible to generate a carpet, though a perverse choice of weighting coefficients could effectively quadratize the spectrum. Similar reasoning suggested why Ψ_{cl} , from Chapter 2, should so often resemble a classically oscillating packet.

Chapter 6

Conclusion

6.1 Results

The principal result of this thesis may be an understanding of how the different elements in a particular problem – potential, eigenfunctions, spectrum, and weighting coefficients – will govern revivals, dephasing, and carpet features. The spectrum is the chief determinant of revival dynamics, though the initial wavefunction and the potential itself govern the spatial distribution of fractional revivals. Though the specifics of dephasing obviously depend on every parameter available, a gross dependence on $1/\Delta n$, where Δn is the spread in weighting coefficients, seemed to be quite general. As for carpet phenomena, we could conclude that the spectrum itself governs the existence of the carpet, insofar as it determines whether the velocity degeneracy condition (Equation 5.13) will be met. The weighting coefficients govern (roughly) which channels and ridges are most pronounced, meaning that if we were to use the same weighting in two iso-spectral problems, we would expect the same number of lines and distribution of line weights. We would not, however, expect the canals and ridges to have the same spatial distribution.

6.2 Prospects for Future Work

Although these results are interesting, they are best seen as a platform from which to launch further work.

Are Carpets only a Semiclassical Phenomenon?

It would appear, from the analysis presented here, that revivals and dephasing are essentially semiclassical phenomena, and that carpets are definitely semiclassical phenomena. This is in part because our analysis has been directed towards those problems from the beginning. It would be interesting to answer conclusively whether a superposition that included a significant weighting of low-energy states could produce any of these effects, or demonstrate similar but distinct phenomena. We would start the hunt with $\Delta n \approx \bar{n} \gg 1$.

More than One Quantum Number

A typical result of increasing the number of quantum numbers in a problem (typically a result of increasing the spatial dimensionality) is a proliferation of energy-degenerate states. It is unclear whether those new energy degeneracies would contribute to the velocity degeneracy that weaves a carpet, or whether their contribution would be unnoticeable. Particularly interesting would be study of the two- or three-dimensional harmonic oscillator, which would introduce rather more velocity degeneracy than we had before.

Beyond Quadratic Potentials

For reasons stated several times, the most important of which is the at-most-quadratic nature of the spectrum high in a well, this analysis has been focused on quadratic potentials. It would be interesting, though, to see how much of our analysis, and how many of the phenomena, carried over into other potentials. This is related to the semiclassical problem – we have many times exploited the fact that the limiting spectrum of any well can't rise any faster than n^2 as a way of avoiding

possibly more interesting (non- n^2) behavior near the bottom of the well.

Open Systems

We have also only considered bound states in this analysis. We would expect that revival phenomena would disappear if probability wasn't being "reflected back" by the walls of the well, but we might see revival-like phenomena for a particle that was escaping its well on a time scale longer than its revival time. Since they appear relatively early in the time-evolution of the particle, we might also see, and perhaps subsequently lose, carpet features.

Fractals, Fractals, Fractals

As I stated in the introduction, I still believe that for those wise in the ways of analysis there is much to be learned from the self-similarity of quantum carpets. The way is far from clear here – perhaps there is a way to go from potential and weighting coefficients to an iterated function system? Measure of the fractal dimension of carpets that are not the square well would be a good start.

Other Equations

I've heard rumor that the Schrödinger equation isn't the only game in town, so far as quantum mechanics goes – for example, the Klein-Gordon equation and the non-linear Schrödinger equation. What sorts of revival phenomena and carpets do these other equations produce? Do the techniques outlined here work there? Related to this, I think, is the application of carpets to BEC. Even if they're not related, the existing papers suggest that this is a topic ready for exploration.

Of course, these techniques may be applied to other wave equations as well. We earlier mentioned the correspondence between these problems and waveguides in EM.

Finding Particular Intermode Traces

One prominent problem in Chapter 5 is the lack of a technique to systematically find the locations of the peaks and valleys that will be expressed in the carpet. This is not an easy problem, and it would be an interesting one to resolve. I suspect that a background in Fourier analysis would be helpful in such an attempt.

Wavepacket Engineering

There has already been a proposal to use our understanding of revival dynamics for the construction of wavepackets with very particular behaviors, [Chen and Yeazell, 1998]. It is not inconceivable that we could take this a step further and, using whatever technique we had to find the exact distribution of peaks and valleys in a carpet, start from the requirement that a wavepacket have certain canals and ridges and come up with a potential and weighting conditions that would produce those features. There does not seem to be, as yet, a burning demand for this, but this does sound vaguely like something that would be of interest in nanofabrication processes.

Appendix A

A Few Exactly Solvable Potentials

In my numerical work on this project I have relied heavily on the following exactly solvable potentials. Knowing the eigenfunctions exactly frees us from the worry that some interesting phenomenon is actually an artifact of our numerical integration of the Schrödinger equation. They allow us to study a variety of systems – harmonic oscillators, anharmonic oscillators, symmetric potentials, non-symmetric potentials, infinite wells, finite wells, double wells, and iso-spectral potentials. These have allowed us to test the impact of various properties of the potential on the dynamics – for example, the observation that iso-spectral potentials could have different spatial symmetries ruled out the idea that one spectrum (or even one spectrum and one set of weighting coefficients) produced one carpet.

In this Appendix, as in the rest of my thesis, I have set $\hbar = 2m = 1$.

A.1 Old Friends

These two potentials are textbook standards – I took them from [Griffiths, 1995, 24-44]. I present them here to make my notation clear.

A.1.1 The Infinite Square Well

The infinite square potential is defined as

$$V(x) = \begin{cases} 0, & 0 \leq x \leq L, \\ \infty, & \text{otherwise.} \end{cases} \quad (\text{A.1})$$

It has a spectrum

$$E_n = \frac{n^2 \pi^2}{L^2}, \quad (\text{A.2})$$

and eigenfunctions

$$\psi_n(x) = \sqrt{\frac{2}{L}} \sin\left(\frac{n\pi}{L}x\right). \quad (\text{A.3})$$

A.1.2 The Simple Harmonic Oscillator

The simple harmonic oscillator potential is

$$V(x) = \frac{1}{2}\omega^2 x^2. \quad (\text{A.4})$$

If we define a dimensionless replacement for x ,

$$\xi = \sqrt{\omega}x, \quad (\text{A.5})$$

we have a spectrum

$$E_n = \left(n + \frac{1}{2}\right)\omega \quad (\text{A.6})$$

and eigenfunctions

$$\psi_n(x) = \left(\frac{\omega}{\pi}\right)^{1/4} (2^n n!)^{-1/2} H_n(\xi) e^{-\xi^2/2}. \quad (\text{A.7})$$

A.2 Cousins from the Old Country

These potentials are all taken from a text on supersymmetric quantum mechanics, [Cooper et al., 2001, 40-41]. They are all, in supersymmetric-parlance, shape invariant potentials – when subjected to the supersymmetry transformation they retain their algebraic form. Many of them make use of the following definitions,

$$\begin{aligned} s_1 &\equiv s - n + a, \\ s_2 &\equiv s - n - a, \\ s_3 &\equiv a - n - s, \\ s_4 &\equiv -(s + n + a). \end{aligned}$$

Each also involves three constants, A , B , and α , along with a few auxiliary functions and constants. One warning about these potentials – they are not normalized, though they are normalizable. What's more, some of them require a bit of numeric finesse – in *Mathematica* 4.0, at least, they begin to oscillate rapidly in regions where they should be falling off exponentially.

A.2.1 The Morse Oscillator

The Morse oscillator potential is

$$V(x) = A^2 + B^2 \exp(-2\alpha x) - 2B \left(A + \frac{\alpha}{2} \right) \exp(-\alpha x) \quad (\text{A.8})$$

and has spectrum

$$E_n = A^2 - (A - n\alpha)^2. \quad (\text{A.9})$$

If we define the auxiliary function and constant

$$y = \frac{2B}{\alpha} e^{-\alpha x}, \quad (\text{A.10})$$

$$s = \frac{A}{\alpha}, \quad (\text{A.11})$$

we can write the eigenfunctions as

$$\psi_n(x) = y^{s-n} \exp\left(-\frac{1}{2}y\right) L_n^{2s-2n}(y). \quad (\text{A.12})$$

The Morse oscillator is iso-spectral with the Pöschl-Teller potential and the Scarf II (hyperbolic) potential.

A.2.2 The Eckart Potential

The Eckart potential is

$$V(r) = A^2 + \frac{B^2}{A^2} - 2B \coth(\alpha r) + A(A - \alpha) \operatorname{cosech}^2 \alpha r \quad (\text{A.13})$$

and has spectrum

$$E_n = A^2 - (A + n\alpha)^2 - \frac{B^2}{(A + n\alpha)^2} + \frac{B^2}{A^2}. \quad (\text{A.14})$$

We define the auxiliary function and constants

$$y = \coth(\alpha r), \quad (\text{A.15})$$

$$s = \frac{A}{\alpha}, \quad (\text{A.16})$$

$$\lambda = \frac{B}{\alpha}, \quad (\text{A.17})$$

$$a = \frac{\lambda}{n + s}, \quad (\text{A.18})$$

and write the eigenfunctions as

$$\psi_n(r) = (y - 1)^{s_3/2} (y + 1)^{s_4/2} P_n^{(s_3, s_4)}(y). \quad (\text{A.19})$$

A.2.3 The Pöschl-Teller Potential

The Pöschl-Teller potential is

$$V(x) = A^2 + (B^2 + A^2 + A\alpha) \operatorname{cosech}^2(\alpha r) - B(2A + \alpha) \coth(\alpha r) \operatorname{cosech}(\alpha r) \quad (\text{A.20})$$

and has spectrum

$$E_n = A^2 - (A - n\alpha)^2. \quad (\text{A.21})$$

We define the auxiliary function and constants

$$y = \cosh(\alpha r), \quad (\text{A.22})$$

$$s = \frac{A}{\alpha}, \quad (\text{A.23})$$

$$\lambda = \frac{B}{\alpha}, \quad (\text{A.24})$$

and write the eigenfunctions as

$$\psi_n(x) = (y - 1)^{(\lambda-s)/2} (y + 1)^{-(\lambda+s)/2} P_n^{(\lambda-s-1/2, -\lambda-s-1/2)}(y). \quad (\text{A.25})$$

The Pöschl-Teller is iso-spectral with the Morse oscillator and the Scarf II (hyperbolic) potential.

A.2.4 The Scarf I (Trigonometric) Potential

The Scarf I (trigonometric) potential is

$$V(x) = -A^2 + (A^2 + B^2 - A\alpha) \sec^2 \alpha x - B(2A - \alpha) \tan(\alpha x) \sec(\alpha x) \quad (\text{A.26})$$

and has spectrum

$$E_n = (A + n\alpha)^2 + A^2. \quad (\text{A.27})$$

Defining the auxiliary function and constants

$$y = \sin \alpha x, \quad (\text{A.28})$$

$$s = \frac{A}{\alpha}, \quad (\text{A.29})$$

$$\lambda = \frac{B}{\alpha}, \quad (\text{A.30})$$

we write the eigenfunctions as

$$\psi_n(x) = (1 - y)^{(s-\lambda)/2} (1 + y)^{(s+\lambda)/2} P_n^{(s-\lambda-1/2, s+\lambda+1/2)}(y). \quad (\text{A.31})$$

A.2.5 The Scarf II (Hyperbolic) Potential

The Scarf II (hyperbolic) potential is

$$V(x) = A^2 + (B^2 + A^2 - A\alpha) \operatorname{sech}^2 \alpha x + 2B(2A + \alpha) \operatorname{sech}(\alpha x) \tanh(\alpha x) \quad (\text{A.32})$$

and has spectrum

$$E_n = A^2 - (A - n\alpha)^2. \quad (\text{A.33})$$

Defining the auxiliary function and constants,

$$y = \sinh \alpha x, \quad (\text{A.34})$$

$$s = \frac{A}{\alpha}, \quad (\text{A.35})$$

$$\lambda = \frac{B}{\alpha}, \quad (\text{A.36})$$

we write the eigenfunctions as

$$\psi_n = i^n (1 + y^2)^{-s/2} \exp(-\lambda \tan^{-1} y) P_n^{(i\lambda-s-1/2, -i\lambda-s-1/2)}(y). \quad (\text{A.37})$$

The Rosen-Morse II (hyperbolic) potential is iso-spectral with the Pöschl-Teller potential and the Morse oscillator.

A.2.6 The Rosen-Morse I (Trigonometric) Potential

The Rosen-Morse I (trigonometric) potential is

$$V(x) = A(A - \alpha) \operatorname{cosec}^2 \alpha x + 2B \cot \alpha x - A^2 + \frac{B^2}{A^2} \quad (\text{A.38})$$

and has spectrum

$$E_n = (A + n\alpha)^2 - A^2 - \frac{B^2}{(A + n\alpha)^2} + \frac{B^2}{A^2}. \quad (\text{A.39})$$

Defining the auxiliary function and constants,

$$y = i \cot \alpha x, \quad (\text{A.40})$$

$$s = \frac{A}{\alpha}, \quad (\text{A.41})$$

$$\lambda = \frac{B}{\alpha^2}, \quad (\text{A.42})$$

$$a = \frac{\lambda}{s + n}, \quad (\text{A.43})$$

we can write the eigenfunctions as

$$\psi_n(x) = (y^2 - 1)^{-(s-n)/2} \exp(a\alpha x) P_n^{(-s-n+ia, -s-n-ia)}(y). \quad (\text{A.44})$$

A.2.7 The Rosen-Morse II (Hyperbolic) Potential

The Rosen-Morse II (hyperbolic) potential is

$$V(x) = -A(A - \alpha) \operatorname{cosech}^2 \alpha x + 2B \cot \alpha x + A^2 + \frac{B^2}{A^2} \quad (\text{A.45})$$

and has spectrum

$$E_n = -(A + n\alpha)^2 + A^2 - \frac{B^2}{(A + n\alpha)^2} + \frac{B^2}{A^2}. \quad (\text{A.46})$$

Defining the auxiliary function and constants,

$$y = \coth \alpha x, \quad (\text{A.47})$$

$$s = \frac{A}{\alpha}, \quad (\text{A.48})$$

$$\lambda = \frac{B}{\alpha^2}, \quad (\text{A.49})$$

$$a = \frac{\lambda}{s + n}, \quad (\text{A.50})$$

we can write the eigenfunctions as

$$\psi_n(x) = (1 - y)^{s_1/2} (1 + y)^{s_2/2} P_n^{(s_1, s_2)}(y). \quad (\text{A.51})$$

Appendix B

Farey Sequences

In a typical revival problem, we will only be able to resolve a certain number of revivals, due to finite packet width. Because of this the pattern of revivals should follow a Farey sequence. The Farey sequence¹ is a simple object: F_n is defined as the sequence (in increasing order) of rational fractions p/q such that $p \leq q$, p and q relatively prime, and $q \leq n$. A few examples,

$$F_3 = \frac{0}{1}, \frac{1}{3}, \frac{1}{2}, \frac{2}{3}, \frac{1}{1}, \tag{B.1}$$

$$F_5 = \frac{0}{1}, \frac{1}{4}, \frac{1}{3}, \frac{2}{5}, \frac{1}{2}, \frac{3}{5}, \frac{2}{3}, \frac{3}{4}, \frac{1}{1}, \tag{B.2}$$

$$F_8 = \frac{0}{1}, \frac{1}{5}, \frac{1}{4}, \frac{2}{7}, \frac{1}{3}, \frac{3}{8}, \frac{2}{5}, \frac{3}{7}, \frac{1}{2}, \frac{4}{7}, \frac{3}{5}, \frac{5}{8}, \frac{2}{3}, \frac{5}{7}, \frac{3}{4}, \frac{4}{5}, \frac{1}{1}. \tag{B.3}$$

If we define Farey addition as

$$\frac{p}{q} \oplus_F \frac{n}{m} = \frac{p+n}{q+m}, \tag{B.4}$$

then starting with one Farey sequence we can generate another Farey sequence by Farey adding each neighboring term in the given Farey sequence. The resulting fractions will already be reduced, and positioned correctly in the sequence.

In Figure B.1 we provide a graph of the first 15 Farey sequences, along with a carpet from the square well and a quantum beats plot.

¹For more on Farey sequences, see [Harter, 2001] or [Weisstein, 1999].

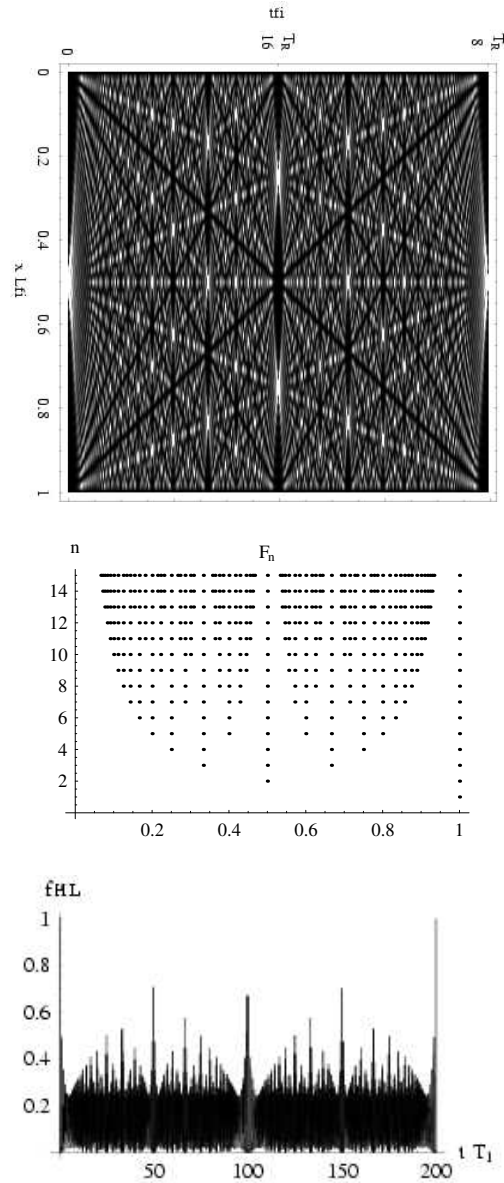


Figure B.1: A plot of the infinite square well (top), with an initial spatial Gaussian wavepacket, $\xi = 1/2$, $\sigma_x = 0.003$, the Farey sequences F_1 through F_{15} (middle), and a two-time-scale quantum beat problem with $T_2/T_1 = 200$, and a Gaussian distribution of P_k with $\sigma_k = 8$ (bottom).

List of Figures

1.1	A particle in the infinite square well. Lighter areas indicate greater probability density. Our initial wavefunction is a Gaussian packet, centered on $x = L/2$, with $\sigma_x = 0.003L$. For the definition of T_R , see Chapter 2.	8
2.1	$\ \Psi\ ^2$ for a particle in an infinite square well, such that $T_R = 80T_{cl}$. The distribution of coefficients is Gaussian, with $\bar{n} = 40$ and $\sigma_n = 2$. For the form of the square well that I am using, see Section A.1.1.	20
2.2	$\ \Psi\ ^2$ for a simple harmonic oscillator. The distribution of coefficients is Gaussian, with $\bar{n} = 6$ and $\sigma_n = 2$. For the version of the simple harmonic oscillator that I am using, see Section A.1.2.	20
2.3	Plots of $\ \Psi\ ^2$ for a particle in an infinite square well at $t = 0$, $t = T_R/2$, and $t = T_R/4$. Note that the scale is different for the rightmost plot – though conservation of probability shrinks our peaks, they have the same shape as the peaks in the other two plots.	20
2.4	Fractional revivals in the infinite square well. Our initial wavefunction is a Gaussian packet, centered on $x = L/2$, with $\sigma_x = 0.003L$. The symmetry of our wavepacket allows it to have a full revival (modulo an overall phase factor) at $t = T_R/8$. At times below that, though, we should be able to count the fractional revivals.	22

2.5 $V(\alpha r)$ (above) and $\|\Psi_{cl}\|^2$ (below) for a particle in the Pöschl-Teller potential (see Appendix A). The dotted line in the above plot indicates $E_{\bar{n}}$, in the lower plot they indicate four different classical paths of energy $E_{\bar{n}}$. The Pöschl-Teller potential has a purely quadratic spectrum. For more details on it, see Section A.2.3. 28

2.6 $V(\alpha x)$ (above) and $\|\Psi_{cl}\|^2$ (below) for a particle in the Morse potential (see Appendix A). The dotted line in the above plot indicates $E_{\bar{n}}$, in the lower plot they indicate four different classical paths of energy $E_{\bar{n}}$. The Morse potential has a purely quadratic spectrum. For more details on it, see Section A.2.1. 28

2.7 Ψ_{cl} for a roughly Gaussian spatial distribution, centered at $x = a/3$ 32

3.1 A Gaussian distribution of the P_k , with $T_2/T_1 = 200$ and $\sigma_n = 8$. In the plot of the early evolution, by Equation 3.29 dephasing should occur at $t \approx 3.125T_1$ 38

3.2 A Gaussian distribution of the P_k , with $T_2/T_1 = 200$ and $N = 8$. In the plot of the early evolution, by Equation 3.53 dephasing should occur at $t \approx 3.125T_1$ 38

3.3 $\text{Re}\{\text{Erf}(\phi x)\}$, $x \in [-10, 10]$ 48

3.4 $\text{Im}\{\text{Erf}(\phi x)\}$, $x \in [-10, 10]$ 48

4.1 These density plots show a solution of the infinite square well in the region $\tau \in [0, 4]$, $\xi \in [0, 1]$ for $\Delta n = 5$, $\bar{n} = 30$. On the left are the five relevant terms from Equation 4.27, on the right are the middle 10 terms of the sum in Equation 4.2. 61

4.2 All of these show the region $\tau \in [0.5, 1.5]$, $\xi \in [0, 1]$ for $\Delta n = 5$, $\bar{n} = 30$, and the time it took *Mathematica* to plot them. On the left is the $l = -1$ term from Equation 4.27, the middle figure contains the middle 20 terms of the sum in Equation 4.2, and at right is a plot of the middle 10 terms from that same Equation. 62

4.3 A plot of $\exp\left(-\frac{y^2}{2\sigma^2}\right)$ (dashed) and $\text{sech}\left(\alpha\frac{y}{2\sigma}\right)$ (solid), $-5\sigma \leq y \leq 5\sigma$. The constant $\alpha = \text{arcsech}\left(\frac{1}{e^2}\right) \approx 2.69$ is chosen so that the two functions are equal at $y = \pm 2\sigma$ 62

4.4 These density plots show a solution of the infinite square well in the region $\tau \in [0, 4]$, $\xi \in [0, 1]$ for $\Delta n = 5$, $\bar{n} = 30$, and the white line indicates the lower of the $A = 1$ solutions of Equation 4.45. On the left are the five relevant terms from Equation 4.27, on the right are the middle 10 terms of the sum in Equation 4.2. Note that the ridges in the left plot only appear above the line, and in the right plot that this holds for $\xi < 1/2$ – for $\xi > 1/2$, the interference between terms in Equation 4.27 becomes non-negligible. 66

5.1 Two plots of the simple harmonic oscillator. On the left, the distribution of coefficients is Gaussian, with $\bar{n} = 6$ and $\sigma_n = 2$, while the plot on the right is an even weighting of the perfect squares between 1 and 81. 75

5.2 The $|v_{nm}| = \pi$ (left) and $|v_{nm}| = 2\pi$ (right) velocity bundles for an even distribution of weighting coefficients between $n = 1$ and $n = 10$ in the infinite square well. 77

5.3 The full carpet, coefficients evenly weighted between $n = 1$ and $n = 10$ 78

5.4 The $v_{nm} = \pi$ intermode terms. Note that they do, indeed, have a period $T = T_R$ 78

5.5 The $v_{nm} = 2\pi$ intermode terms. Note that they have a period $T = T_R/2$ 78

5.6 Plots of Ψ_{cl} in two potentials, one with a quadratic spectrum and one with a non-quadratic spectrum. On the left is the Morse Potential, with $E_n = A^2 - (A - \alpha n)^2$, and on the right the Rosen-Morse I potential, with $E_n = -A^2 + (A + \alpha n)^2 - (B/(A + \alpha n))^2 + (B/A)^2$. In both cases A , B , and α are independent constants. The black lines overlaying the maxima are classical paths for those potentials with $E = E_{\bar{n}}$. For more on these potentials, see Sections A.2.1 and A.2.6. 81

B.1 A plot of the infinite square well (top), with an initial spatial Gaussian wavepacket, $\xi = 1/2$, $\sigma_x = 0.003$, the Farey sequences F_1 through F_{15} (middle), and a two-time-scale quantum beat problem with $T_2/T_1 = 200$, and a Gaussian distribution of P_k with $\sigma_k = 8$ (bottom). 96

Bibliography

- [Abramowitz and Stegun, 1965] Abramowitz, M. and Stegun, I. A. (1965). *Handbook of mathematical functions*. Dover.
- [Aronstein, 2000] Aronstein, D. L. (2000). Analytical investigation of revival phenomena in the finite square-well potential. *Physical Review A*, 62:022102.
- [Aronstein and Stroud, 1997] Aronstein, D. L. and Stroud, C. R. J. (1997). Fractional wave-function revivals in the infinite square well. *Physical Review A*, 55(6):4526–4537.
- [Averbukh and Perelman, 1989] Averbukh, I. S. and Perelman, N. (1989). Fractional revivals: Universality in the long-term evolution of quantum wave packets beyond the correspondence principle dynamics. *Physics Letters A*, 139(9):449–453.
- [Averbukh and Perelman, 1991] Averbukh, I. S. and Perelman, N. (1991). The dynamics of wave packets of highly-excited states of atoms and molecules. *Sov. Phys. Usp.*, 34(7):572–591.
- [Berry, 1996] Berry, M. V. (1996). Quantum fractals in boxes. *Journal of Physics A: Mathematical and General*, 29:6617–6629.
- [Berry and Bodenschatz, 1999] Berry, M. V. and Bodenschatz, E. (1999). Caustics, multiply reconstructed by talbot interference. *Journal of Modern Optics*, 46(2):349–365.
- [Berry and Klein, 1996] Berry, M. V. and Klein, S. (1996). Integer, fractional, and fractal talbot effects. *Journal of Modern Optics*, 43(10):2139–2164.

- [Bluhm et al., 1996] Bluhm, R., Kostelecky, V. A., and Porter, J. A. (1996). The evolution and revival structure of quantum wave packets. *American Journal of Physics*, 64:944.
- [Chen and Yeazell, 1998] Chen, X. and Yeazell, J. A. (1998). Analytical wave-packet design scheme: Control of dynamics and creation of exotic wave packets. *Physical Review A*, 57(4):R2274–R2277.
- [Choi et al., 2001] Choi, S., Burnett, K., Friesch, O. M., Kneer, B., and Schleich, W. (2001). Spatiotemporal interferometry for trapped atomic bose-einstein condensates. *Physical Review A*, 63:065601.
- [Cooper et al., 2001] Cooper, F., Khare, A., and Sukhatme, U. (2001). *Supersymmetry in Quantum Mechanics*. World Scientific Publishing Co.
- [Courant and Hilbert, 1953] Courant, R. and Hilbert, D. (1953). *Methods of mathematical physics*. Interscience Publishers, New York, 1st english edition.
- [Dubra and Ferrari, 1999] Dubra, A. and Ferrari, J. A. (1999). Diffracted field by an arbitrary aperture. *American Journal of Physics*, 67(1):87–92.
- [Friesch et al., 2000] Friesch, O., Marzoli, I., and Schleich, W. P. (2000). Quantum carpets woven by wigner functions. *New Journal of Physics*, 2(4):4.1–4.11.
- [Griffiths, 1995] Griffiths, D. J. (1995). *Introduction to quantum mechanics*. Prentice Hall, Englewood Cliffs, N.J.
- [Grossmann et al., 1997] Grossmann, F., Rost, J.-M., and Schleich, W. P. (1997). Spacetime structures in simple quantum systems. *Journal of Physics A: Mathematics and General*, 30:L277–L283.
- [Hall et al., 2001] Hall, M. J., Reineker, M. S., and Schleich, W. P. (2001). Unravelling quantum carpets: A travelling wave approach. *arXiv*, (quant-ph/9906107 v2).
- [Harter, 2001] Harter, W. G. (2001). Quantum-fractal revival structure in cn quadratic spectra: Base-n quantum computer registers. *Physical Review A*, 64:012312–1.

- [Jie et al., 1998] Jie, Q.-L., Wang, S.-J., and Wei, L.-F. (1998). Partial revivals of wave packets: An action-angle phase-space description. *Physical Review A*, 57(5):3262–3267.
- [Kaplan et al., 2000] Kaplan, A., Marzoli, I., Lamb, W. J., and Schleich, W. (2000). Multimode interference: Highly regular pattern formation in quantum wave-packet evolution. *Physical Review A*, 61:032101.
- [Kaplan et al., 1998] Kaplan, A., Stifter, P., van Leeuwen, W., Lamb, W. J., and Schleich, W. P. (1998). Intermode traces-fundamental interference phenomenon in quantum and wave physics. *Physica Scripta*, T76:93–97.
- [Knospe and Schmidt, 1996] Knospe, O. and Schmidt, R. (1996). Revivals of wave packets: General theory and application of rydberg clusters. *Physical Review A*, 54(2):1154–1160.
- [Leichtle et al., 1996a] Leichtle, A., Averbukh, I. S., and Schleich, W. (1996a). Generic structure of multilevel quantum beats. *Physical Review Letters*, 77(19):3999–4002.
- [Leichtle et al., 1996b] Leichtle, C., Averbukh, I. S., and Schleich, W. (1996b). Multilevel quantum beats: An analytical approach. *Physical Review A*, 54(6):5299–5312.
- [Lock and Andrews, 1992] Lock, J. A. and Andrews, J. H. (1992). Optical caustics in natural phenomena. *American Journal of Physics*, 60(5):397–407.
- [Loinaz and Newman, 1999] Loinaz, W. and Newman, T. (1999). Quantum revivals and carpets in some exactly solvable systems. *Journal of Physics A: Mathematics and General*, 32:8889–8895.
- [Marzoli et al., 1998a] Marzoli, I., Bialynicki-Biruli, I., Friesch, O., Kaplan, A., and Schleich, W. (1998a). The particle in the box: Intermode traces in the propagator. *arXiv*, (quant-ph/9804015).
- [Marzoli et al., 1998b] Marzoli, I., Saif, F., Bialynicki-Birula, I., Friesch, O., Kaplan, A., and Schleich, W. (1998b). Quantum carpets made simple. *Acta Physica Slovaca*, 48(3):323–333. Wigner Functions.

- [Nieto and Simmons, 1979] Nieto, M. M. and Simmons, L. J. (1979). Limiting spectra from confining potentials. *American Journal of Physics*, 47(7):634–635.
- [Provost and Baranger, 1993] Provost, D. and Baranger, M. (1993). A semiclassical calculation of scars for a smooth potential. *arXiv*, (chao-dyn/9305003).
- [Razi Naqvi et al., 2001] Razi Naqvi, K., Waldenstrom, S., and Haji Hassan, T. (2001). Fractional revival of wave packets in an infinite square well: a fourier perspective. *European Journal of Physics*, 22:395–402.
- [Rozmej and Arvieu, 1998] Rozmej, P. and Arvieu, R. (1998). Clones and other interference effects in the evolution of angular-momentum coherent states. *Physical Review A*, 58(6):4314–4329.
- [Ruostekoski et al., 2001] Ruostekoski, J., Kneer, B., Schleich, W. P., and Rempe, G. (2001). Interference of a bose-einstein condensate in a hard-wall trap: From the nonlinear talbot effect to the formation of vorticity. *Physical Review A*, 63:043613.
- [Saif, 2000] Saif, F. (2000). Quantum recurrences: Probe to study quantum chaos. *Physical Review E*, 62(5):6308–6311.
- [Silverman, 1995] Silverman, M. P. (1995). *More than one mystery : explorations in quantum interference*. Springer-Verlag, New York.
- [Weisstein, 1999] Weisstein, E. W. (1999). Farey sequences. <http://mathworld.wolfram.com/FareySequences.html>.
- [Wojcik et al., 2000] Wojcik, D., Bialynicki-Birula, I., and Zyczkowski, K. (2000). Time evolution of quantum fractals. *Physical Review Letters*, 85(24):5022–5025.
- [Wojcik and Zyczkowski, 2001] Wojcik, D. and Zyczkowski, K. (2001). Fractality of certain quantum states. *arXiv*, (math-ph/0107030).
- [Wolfram, 2002] Wolfram (2002). The error function. <http://functions.wolfram.com/GammaBetaErf/Erf/>.

- [Wright et al., 1997] Wright, E. M., Wong, T., Collett, M. J., Tan, S. M., and Walls, D. F. (1997). Collapses and revivals in the interference between two bose-einstein condensates formed in small atomic samples. *Physical Review A*, 56(1):591–602.